2-25-2013

Statistical Study of Ground Motion Amplification in the Mississippi Embayment

Mojtaba Malekmohammadi

STATISTICAL STUDY OF GROUND MOTION AMPLIFICATION IN THE MISSISSIPPI EMBAYMENT

by

Mojtaba Malekmohammadi

A Dissertation

Submitted in Partial Fulfillment of the

Requirements for the Degree of

Doctor of Philosophy

Major: Civil Engineering

The University of Memphis

May 2013

To Mom and Dad

ACKNOWLEDGMENTS

I would like to thank Dr. Shahram Pezeshk for his dedication and support during my doctoral studies. His knowledge and experience have greatly contributed to my academic pursuits. I will always appreciate what you have helped me accomplished. I also would like to thank my committee members, Professors: David Arellano, Oliver Boyd, Charles Camp, and Chris Cramer for all their help and comments that improved the quality of this study.

I also wish to acknowledge Fabian Bonilla, Walter Silva, Dominic Assimaki, Arash Zandieh, and Wei Li for providing the computer programs used in this study as well as the NGA-East working group for sharing the database with us.

ABSTRACT

Malekmohammadi, Mojtaba. Ph.D. The University of Memphis. May 2013. Statistical study of ground motion amplification in the Mississippi embayment. Major Professor Shahram Pezeshk, Ph.D.

Three important topics have been studied in this dissertation. First, the effects of deep soil deposits of the Mississippi embayment in ground motion amplification have been studied. Using the results of one-dimensional analyses, a parametric model is developed for the region to estimate the ground motion amplification. The averaged shear-wave velocity in the upper 30 meter, V_{s30}, ranging from 220 to 800 *m/s* and deposit thickness varying from 70 to 750*m,* are considered in the estimation of the ground motion amplification with respect to a generic bedrock profile of the Mississippi embayment. Results indicate that site factors suggested by seismic codes cannot capture the site properties of the Mississippi embayment and are not appropriate for the region.

In the second part, a new step-by-step method is developed to select a set of ground motions which takes into account a site-specific Probabilistic Seismic Hazard Analysis (PSHA) and the associated uncertainties through the defined logic tree. In the proposed method, after capturing the variability of the Uniform Hazard Response Spectrum (UHRS), I used a Monte Carlo procedure to produce a set of response spectra that has mean equals to the target and variability close to the variability of the target at all the spectral periods. Each member of the generated set is called individual target response spectra, and ground motions from the database of real data and also synthetic ground motions are selected based on their similarity with the individual target response spectra. The method's procedure is defined through studying a sample site in North of the Mississippi embayment.

In the last part of the study I developed a model for the ratio of Vertical to Horizontal component of earthquakes (V/H ratio) for the Mississippi embayment. This model can be used in developing the site-specific vertical design spectrum for the region by scaling the horizontal design spectrum resulting from a PSHA. The input parameters of the applied functional form are magnitude, distance, and V_{s30}. The proposed model has the advantage of including site response of the study area.

PREFACE

Three papers resulting from my Ph.D. research are used as the manuscript of this dissertation as Chapters 2, 3, and 4. Articles were submitted to the *Journal of Earthquake Spectra* and the *ASCE Journal of Structural Engineering* and are currently under review. Following is a list of the articles used as chapters in this document:

Chapter 2: Malekmohammadi, Mojtaba, and S. Pezeshk (2012). Ground Motion Amplification Factors for Sites Located within the Mississippi Embayment with Consideration for Deep Soil Deposit, submitted to the *Journal of Earthquake Spectra*.

Chapter 3: Malekmohammadi, Mojtaba, and S. Pezeshk (2012). Capturing Uncertainty in Ground Motion Selection and Scaling, submitted to the *ASCE Journal of Structural Engineering*.

Chapter 4: Malekmohammadi, Mojtaba, and S. Pezeshk (2012). Vertical to Horizontal Ratio Model for the Mississippi Embayment, submitted to the *Journal of Earthquake Spectra.*

TABLE OF CONTENTS

LIST OF TABLES

LIST OF FIGURES

1 Introduction

This research deals with three important topics in the field of site-specific studies: vertical design spectrum, ratio of vertical to horizontal component of earthquakes, ground motion amplification models, and ground motion selection for time-history analysis. The main focus of this dissertation is the Mississippi embayment in the Central United States which is among the areas with high levels of seismic activity in the United States. Deep soil deposits with varying thicknesses along with the high seismic hazard levels make the Mississippi embayment an unique area for research in the field of geotechnical seismic engineering and engineering seismology.

In this dissertation, three important topics in the field of geotechnical engineering and engineering seismology are covered. First, the effects of deep soil deposits of the Mississippi embayment in ground motion amplification have been studied. The Mississippi embayment, which generated three large events in 1811-1812 with estimated moment magnitude of 7.3 to 7.8 (Bakun and Hopper 2004; Cramer and Boyd 2012), extends from southeastern Illinois to the Gulf of Mexico. The goal of this part of the study is to investigate the nonlinear ground motion amplification (or de-amplification) for sites located within the Mississippi embayment due to geology, depth of sediment, and the average shear-wave velocity at the upper 30*m,* as well as earthquake properties such as the peak ground acceleration at the bedrock. The nonlinear response of the soil column is computed using the computer program NOAH which takes into account the pore water pressure development in the soil media. The top 30*m* shear-wave velocity ranging from 220 *m/s* to 800 *m/s* and deposit thickness varying from 70*m* to 750*m* are considered in the estimation of the ground motion amplification with respect to a generic

bedrock profile of the Mississippi embayment with a shear-wave velocity of *3,000 m/s*. Propagated ground motions are simulated using the stochastic point-source method due to a lack of ground motions with engineering significance in the study area. Using the results of one-dimensional analyses for different input ground motions, depth of soil deposits, geology, and shear-wave profiles, a model is developed for the region to estimate the ground motion amplification. To illustrate the strength and the limitations of this study, the proposed model is compared with the NEHRP coefficients and other available studies on site amplification.

The second part of this dissertation is focused on ground motion selection for time-history analysis of structures. Selection of ground motions is a key step in the time-history analysis of special structures, and yet there are limited procedures and recommendations available in the literature on details of the selection and scaling process. In the time-history structural analysis, the structural engineer needs to select ground motions where their response spectrum matches an appropriate target spectrum that is usually a Uniform Hazard Response Spectrum (UHRS) obtained from a Probabilistic Seismic Hazard Analysis (PSHA). In this part of the study, a new step-by-step method is developed to select a set of ground motions which takes into account a site-specific PSHA and the associated uncertainties through the defined logic tree. The logic tree for the sample site consists of two different GMPEs (Tavakoli and Pezeshk 2005; Campbell 2003) as well as five locations for the New Madrid faults as proposed by the U.S. Geological Survey.

In the proposed method after capturing the variability of the UHRS, a Monte Carlo procedure is used to produce a set of response spectra that has the mean and the

variability of the target at all the spectral periods. Each member of the generated set is called individual target response spectra, and ground motions from different databases are selected based on their similarity with the individual target response spectra. As seed earthquakes, acceleration time-histories are selected from the database of real ground motions, earthquakes are produced using a point-source stochastic procedure (the SMSIM computer program), and records are generated using a stochastic finite-fault model (the EXSIM computer program). The strengths and the limitations of the procedure are defined by studying an example site located in the Mississippi embayment.

In the last part of this dissertation, a model for the ratio of vertical to horizontal component of earthquakes (V/H ratio) for the Mississippi embayment is developed. This model can be used in developing the site-specific vertical design spectrum for the region by scaling the horizontal design spectrum resulting from a PSHA. Actual data from two different sources are used in developing the V/H ratio spectrum for the study area; data from the Center for Earthquake Research and Information (CERI) at The University of Memphis, as well as data from the Next Generation Attenuation database developed for the Central and Eastern United States (NGA-East) are used in this research. The input parameters of the applied functional form are magnitude, distance, and the averaged shear-wave velocity in the upper 30 meter, V_{s30}. The proposed model has the advantage of including site response of the study area.

2 Ground Motion Site Amplification Factors Located within the Mississippi Embayment with Consideration of Deep Soil Deposit

2.1 Introduction

The determination of seismic forces applied to typical structures in most seismic design codes are based on a 5% damped design response spectrum. The design spectrum for a given site is typically obtained from a uniform hazard spectrum at the rock level and is modified by site factors to consider soil effects. In the National Earthquake Hazards Reduction Program (NEHRP) *Recommended Provisions for Seismic Regulations for New Buildings and Other Structures, Part 1: Provisions* and *Part 2: Commentary,* ground motion amplification factors are formulated on the basis of the site category which is related to the average shear-wave velocity at the upper 30*m* of soil (V_{s30}). The ordinate of response spectrum at the ground surface is obtained by multiplying the rock response spectrum by a set of soil amplification factors which are dependent on the V_{s30} of the site.

The NEHRP site factors were developed using empirical data from the 1989 Loma Prieta earthquake and also the analytical site response analyses using a series of one-dimensional equivalent linear and nonlinear site response analyses (Dobry *et al*. 2000; Choi and Stewart 2005). The NEHRP site amplifications are defined as the ratio of the Fourier spectral acceleration of motion at the soil surface to the Fourier spectral of the motion at the San Francisco bay area bedrock. A number of studies questioned the validity of the NEHRP site coefficients for other regions, especially regions with thick deposit of soil such as the Mississippi embayment (*e.g.*, Field 2000; Stewart et al. 2003; Choi and Stewart 2005; Borcherdt 2002a and b; Park and Hashash 2004). Results of these studies show that the site amplification of a ground motion is dependent on both the

dynamic properties of the soil and the database of ground motions used in the evaluation of site amplification factors.

There are different ways to estimate the site-specific ground motion amplification factors. One approach to calculate the ground motion amplification for a given area is to use the actual time-histories of earthquakes that occurred in the study area. The ground motion amplification can be calculated by observing the earthquake's time-history at a nearby rock outcrop and compare it to the earthquake's time-history obtained at the study site. In the absence of ground motions of engineering significance, in this study I used the computer program SMSIM (available online at http://www.daveboore.com/software_online.html), which is based on the stochastic point-source model, to compute the input ground motions at the surface of the reference bedrock (V_s = 3,000 *m/s*) for the Mississippi embayment using the seismological parameters of the region. Because of its simplicity and success, the point-source stochastic method is now widely used to predict ground motions in many regions of the world where the number of ground motion recordings is limited and no empirical ground motion relations are available. For this study, I generated 55 input ground motions for site response analyses with *PGA*s ranging from 0.01*g* to 0.90*g*. The stochastic point-source model has been validated in various studies (*e.g.*, Hanks and McGuire 1981; Boore 1983; McGuire et al. 1984; Boore and Atkinson 1987; Toro and McGuire 1987; Silva et al. 1997) and provides reasonable estimates of the acceleration time-history and response acceleration.

2.2 Methodology

In general, the amplification of ground motion is defined as the ratio of any intensity measure of the motion measured at the soil surface to the associated value at the bedrock. In this research, the ground motion amplification for each period is defined as the ratio of spectral acceleration of the motion at the soil surface to the spectral acceleration of the motion at the generic bedrock with a shear-wave velocity of V_s = 3,000 *m/s*:

$$Amp(T) = \frac{SA_{Soil}(T)}{SA_{Rock}(T)} \quad (1)$$

where $SA_{Soil}(T)$ and $SA_{Rock}(T)$ are the values of acceleration response spectrum of the motion at the soil surface and at the bedrock for the spectral period *T*, respectively. Each input ground motion in the database is propagated through different site depths using a one-dimensional nonlinear analysis and ground motion amplification is calculated at spectral periods of 0.0 (or *PGA)*, 0.2, 1.0 and 5.0 seconds. Sites are considered to have soil deposit depths of 70, 140, 400, and 750*m* above the generic bedrock. For each depth and each ground motion in the database, 60 sets of probabilistically generated soil profiles are generated to estimate the soil response to capture the variability in the soil properties. The effect of geologic structure is considered by using two generic soil profiles developed by Romero and Rix (2001) in simulation of soil profiles. Proposed profiles (Uplands and Lowlands) are used as the base profile to randomize soil profiles.

Considering all different soil deposit thicknesses, shear-wave profiles, ground motion *PGA*s, and geologic structures, more than 12,000 nonlinear site response analyses are conducted in this research. Each site response analysis on a PC with dual processor of 3.16 GHz takes an average of 10 minutes. For this study I used the high performance

computing facility at the University of Memphis to conduct site response analyses. The generated data are used to fit a parametric model to predict the soil response for sites located within the Mississippi embayment.

2.3 Ground Motion Database

The ground motion database used in this study consists of input motions simulated using the computer program SMSIM with the moment magnitudes ranging from 4 to 8 and eleven epicentral distances ranging from 10 to 1000 *km*. Silva et al. (1999) and Walling et al. (2008) used the synthetic ground motion in evaluating site responses for the Western United States. Walling *et al.* (2008) used a fixed moment magnitude of 6.5 and different epicentral distances to simulate a range of intensities ground motions at the bedrock. In this study, I selected magnitudes and distances in a way so that the generated ground motions have evenly distributed *PGAs* from small to large.

The simulated ground motions have *PGA*s varying from *0.0001g* to *0.9g*. The input parameters for the SMSIM computer program are adopted from Campbell and Bozorgnia (2008) and Boore and Atkinson (2006). I used a stress drop of 140 bars, *Kappa* value of 0.005 seconds, and the quality factor of $Q=max\ (1000,\ 893f^{0.32})$ to simulate ground motions for the Mississippi embayment. The seismological parameters used in this study are summarized in Table 2-1.

Table 2-1. Seismological parameters used in this study.

Parameter	Value
Magnitude	4, 5, 6, 7, and 8
Distance	10, 25, 50, 75, 100, 150, 200, 300, 500, 750, and 1000 *km*
Shear-wave velocity (depth is variable)(β)	3.0 *km/sec*
Bedrock Density	2.8 g/cm^3
Rupture propagation speed	0.8 β
Stress parameter	140 bars
Kappa	0.005
Geometric Spreading R^b, b =	-1.3(0-70 *km*) +0.2(70-140 *km*) -0.5(>140 *km*)
Distance dependence of duration	0.0 (0-10 *km*) +0.16(10-70 *km*) -0.03(70-130 *km*) +0.04(>140 *km*)
Quality factor	$Q = \max(1000, 893 f^{0.32})$

2.4 Site Response Analysis

Among the available programs for site response analysis, the most widely used is perhaps the SHAKE91 computer program (Idriss and Sun 1992; Cramer 2006; Hartzel et al. 2005; Wen and Wu 1999). The program employs the equivalent linear method to compute the response of horizontally layered soil deposits underlain by horizontal bedrock. The computer program SHAKE91 and the other linear equivalent methods in general have the disadvantage of underestimating ground motions at short periods for thick deposits (Romero and Rix 2001). The basic approach used in this study is to perform one-dimensional site-response analyses using the program NOAH (NOnlinear Anelastic Hysteretic). NOAH is a finite difference procedure formulated by Bonilla et al. (1998) and Bonilla (2000) written in FORTRAN which compute the one-dimensional

nonlinear wave propagation in saturated deep-soil deposits. Equations implemented in the NOAH program were developed by Towhata and Ishihara (1985) that compute nonlinear effects of soil layers such as anelasticity, hysteretic behavior, and generation of pore water pressure. Stress-strain space of soil materials subjected to cyclic loads are among the main dynamic properties of soil which is presented in the form of the hyperbolic model in the NOAH program. Hyperbolic model is a modification of extended Masing rules also known as MKZ rules (Vucetic 1990; Kramer 1996). There are some problems associated with the conventional Masing rule; most notably is the inadequacy of the Masing rule in describing the hysteretic behavior of complicated signals (Li and Liao 1993). Another advantage of NOAH is the calculation of the liquefaction front in the soil media which considers the decrease of effective mean stress due to the increase of pore water pressure in saturated soil layers. The basis of the formulation implemented in the NOAH program is the assumption of the correlation between pore water pressure and shear strength presented by Towhata and Ishihara (1985). Any numerical estimation of nonlinear wave propagation has to comply with the so-called stability conditions. There are numerical constraints on how to discretize the problem in the time and space domain so that the solution converges to the analytical answer. Another companion computer code which is called PRENOAH is used to discretize the variables associated with time and space in a way to ensure stability in NOAH. NOAH's input and output format is modified to run in a batch format for a set of input ground motions and soil layers.

Assimaki and Li (2012) compared three different site response models and proposed a method to estimate the error associated with each model when nonlinear soil

effects are not accounted for. They assumed that the nonlinear site response analysis results is a true estimation of the site response, and used it as a benchmark to evaluate errors associated with the linear visco-elastic and the equivalent linear model. To better illustrate the effects of the site response model on the prediction of surface ground motion, I calculated the site response of a sample site with two layers of soil deposits and total thickness of 70*m* on the top of the bedrock. Table 2-2 summarizes site, soil, and dynamic properties of the sample site used in the example. This site is only used to compare different site response models and the values presented in Table 2-2 do not represent sites used in actual site response analyses. Figure 2-1 shows site response calculated for two different ground motions (top) calculated by three site response computer programs (bottom): NOAH, SHAKE91, and Assimaki and Li (2012). Details on the input and procedure of SHAKE91, NOAH, and the nonlinear model can be found in Idriss and Sun (1992), Bonilla (2000), and Assimaki and Li (2012), respectively. As reflected in Figure 2-1, the mismatch between site responses calculated by SHAKE91 and the other two nonlinear soil response analyses increase (especially at periods less than 2 sec) with the increase in the intensity of the ground motion. SHAKE91, which is an equivalent linear method, has lower values of spectral acceleration at short periods in comparison with the other two nonlinear methods. It is important to note that the site effect can be divided into the response of soil column, basin effects, and topographic effects. The basin effect and topographic effects are considered to be small in the Mississippi embayment (Park and Hashash 2004) and are not addressed and calculated in this study.

Table 2-2. Properties of the sample site used in the comparison of site response models.

	$V_s(m/s)$	Density(kg/m^3)	Thickness(m)	G/ G_{max}	Damping
layer 1	213	1900	30	EPRI	EPRI
layer 2	883	1900	40	EPRI	EPRI
bedrock	3000	2200	NA	EPRI	EPRI

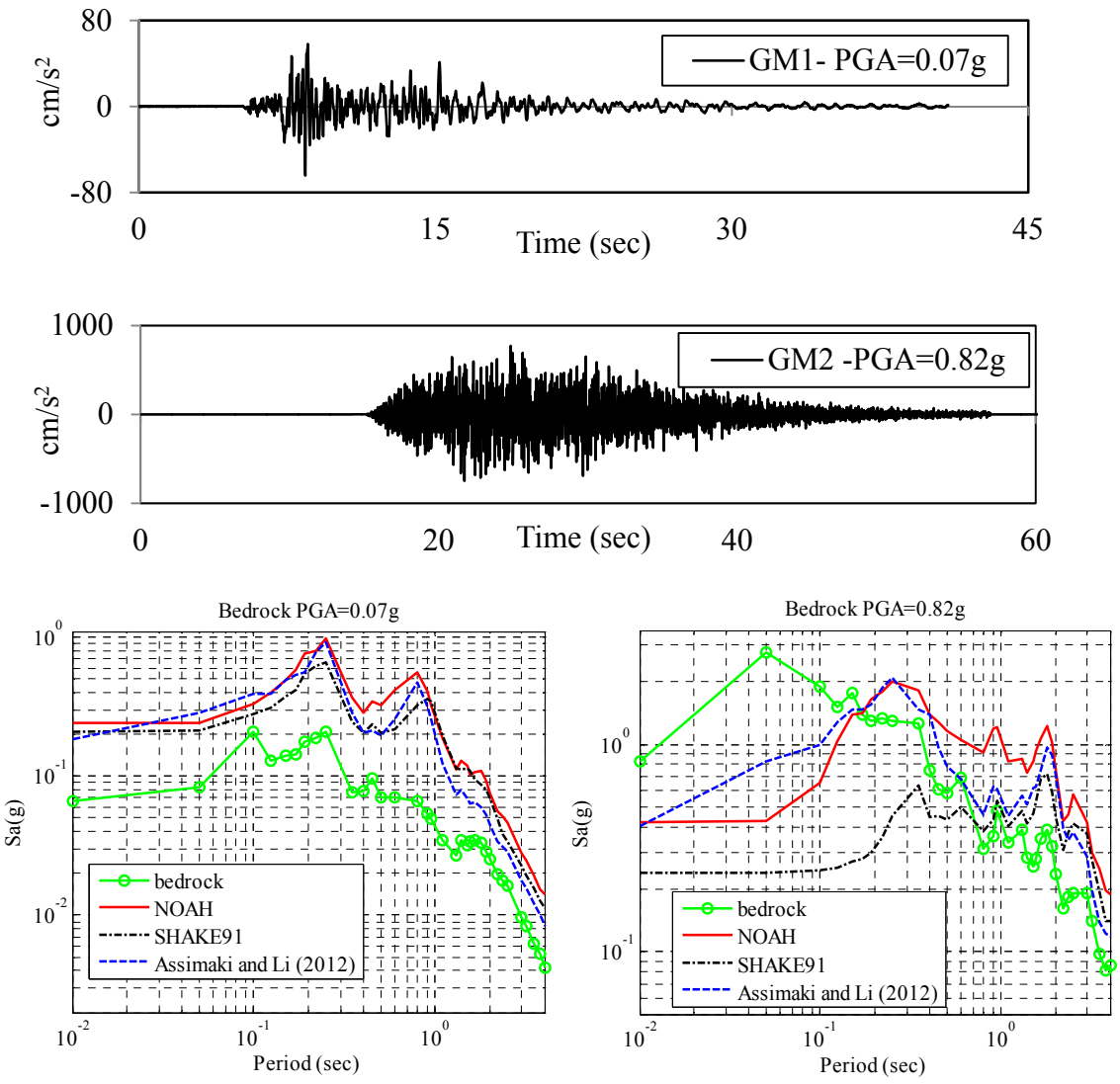

Figure 2-1. Comparison of the computer programs NOAH, SHAKE91, and Assimaki and Li (2012). Site response is calculated for high and low levels of shaking and for a 70m two layered soil deposit.

2.5 Study Area

This study is focused on the Mississippi embayment which has high level of seismicity in the central and Eastern United States. The Mississippi embayment, which extends from southern Illinois to the Mexican gulf, is a wedge-shape geologic structure along the Mississippi river with thicknesses of soil deposits varying from a few meters at the edges to approximately 1,000*m* around the Memphis metropolitan area (see Figure 2-2).

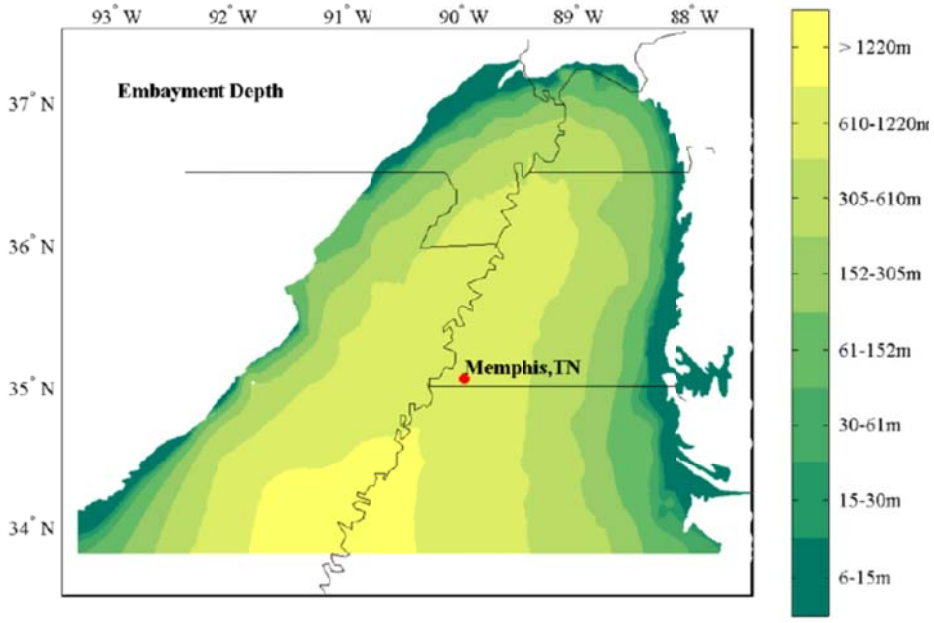

Figure 2-2. Boundary of the Mississippi embayment as well as thickness to Paleozoic rock (Leon 2007).

The shallow slope of bedrock below the Mississippi embayment reduces basin effects and makes the one-dimensional site response analysis appropriate for the study region. One-dimensional analysis is based on the assumption that the response of the soil

deposit is mainly caused by the SH waves propagating vertically from the bedrock. This assumption is true when all layers are horizontal and shallower soil layers have lower values of shear-wave velocities (Kramer 1996). The main focus of this study is the upper Mississippi embayment, which hosts the New Madrid seismic zone (NMSZ). Figure 2-2 shows the thickness of soil layers and the border of the Mississippi embayment.

2.6 Soil Properties

2.6.1 Geology of the Region

Romero and Rix (2001) divided the Mississippi embayment into two geologic structures: Pleistocene-age deposits which is called Uplands and Holocene deposits which is called Lowlands. The Pleistocene-age deposits (Uplands) are found in the interfluve, terrace regions and are characterized by a layer of loess near the surface. Loess deposits are clayey to sandy silt in Tennessee with a maximum thickness of 30*m* along the bluffs of the Mississippi River and thinning eastward (Miller et al. 1966). In the Mississippi embayment, geologic maps classify these deposits as predominantly silt with some deposits from the Eocene (Tertiary) series (Bicker 1969, Romero and Rix 2001). Pleistocene-age deposits were subdivided based on the relative elevation and geographic location. In contrast to Holocene-age deposits (Lowlands), Pleistocene age deposits are more variable in shear-wave velocity and layer thickness. Holocene deposits are mainly found along the floodplains of the Mississippi River and its tributes as alluvium and are divided into deposits within the Mississippi River floodplain and deposits in the floodplain of minor rivers such as the Wolf River and Big Creek. Both of the Uplands and Lowlands have low shear-wave velocity compared to the bedrock of the region, but the generic soil profiles proposed for Lowlands (Romero and Rix 2001, Park

and Hashash 2005) have relatively higher shear-wave velocity up to the depth of 70*m* in comparison with Uplands structure. Below that depth Uplands and Lowlands have the same shear-wave velocity.

2.6.2 Dynamic Soil Properties: G/G_{max} and Damping Ratio vs. Shear Strain

Shear modulus degradation (G/G_{max}) and hysteretic damping ratio vs. shear strain are the key properties in the calculation of the site response at a site. In deep soil deposits, such as the Mississippi embayment, the overburden pressure plays an important role on dynamic soil properties. Generally soils display stiffer characteristics with increase in the depth. EPRI (1993) proposed a set of depth dependent generic G/G_{max} and damping ratio vs. shear strain curves for the Central United States. These curves are plotted in Figure 2-3. EPRI (1993) shear modulus and damping curves have been used in the estimation of the site response in numerous studies (*e.g.*, Park and Hashash 2005; Romero and Rix 2005; Toro and Silva 2001). In the absence of a better estimate of dynamic soil properties for the study area, I used G/G_{max} and damping vs. shear strain of EPRI (1993). Park and Hashash (2004) argued that it is not possible to assign variability parameters for the randomization process due to the lack of laboratory data. Therefore, I did not randomize the dynamic soil properties in performing the site response analysis.

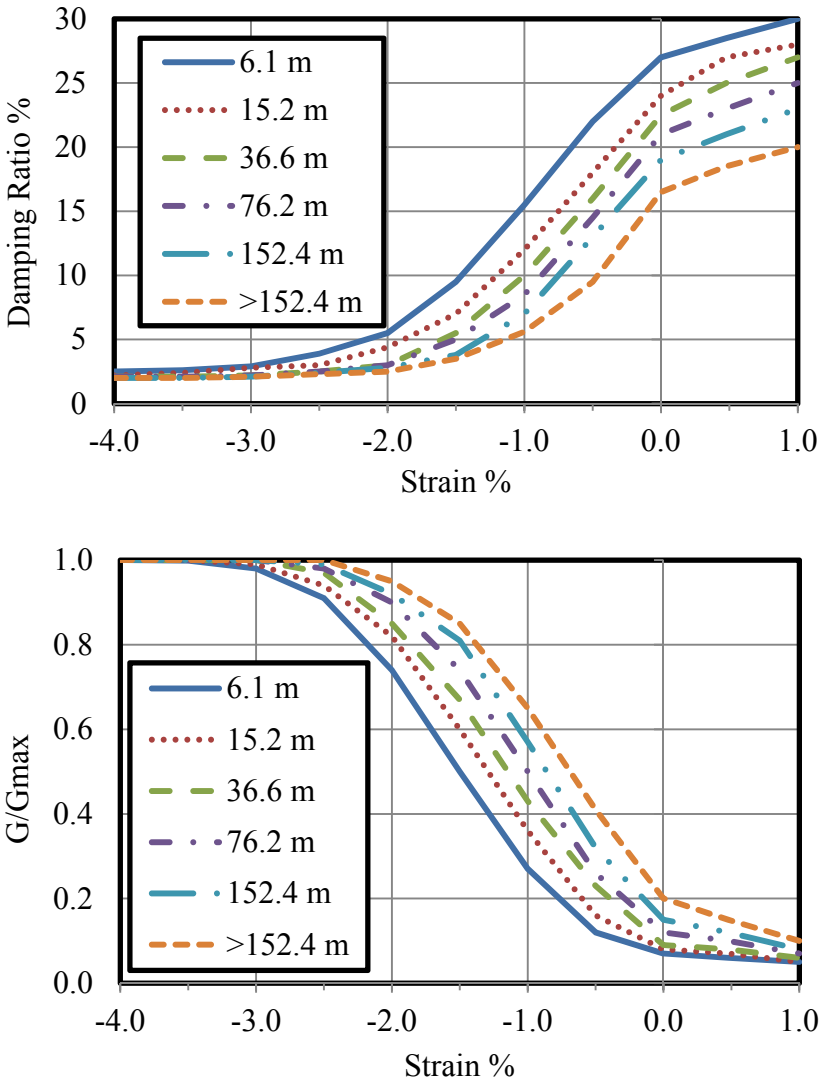

Figure 2-3. Depth dependent dynamic soil properties, damping ratio curves (top) and shear modulus degradation (bottom), proposed by EPRI (1993) used in the site response analyses.

2.6.3 Shear-Wave Velocity

The shear-wave velocity of shallow soil plays a significant role on ground motion characteristics measured at the surface. In the absence of generic soil profiles, I selected the calibration sites compiled by Stewart and coworkers as the base profile for the upper 30*m* shear-wave (http://cee.ea.ucla.edu/faculty/CalibrationSites/Webpage/main.htm).

To have amplification factors reflecting the general properties of the study area, I used the Romero and Rix (2001) generic soil profile for the depths below 30*m* to the bedrock. Romero and Rix (2001) compared several shear-wave velocity profiles in the region and compiled generic shear-wave velocity profiles for Uplands and Lowlands geologic structure. I used four different bedrock depths of 70, 140, 450, and 700*m* to calculate the site response. For each depth, I conducted a series of site response analyses using soil profiles simulated from both Uplands and Lowlands generic soil profiles to investigate the effects of geology as well as the effects of soil depth on the ground motion amplification. In this study, I used V_s = 3,000 *m/s* as the shear-wave velocity of the reference rock, following the recommendation of the Geotechnical Working Group of the Next Generation Attenuation (NGA)-East. Silva et al. (1999) and Kwok and Stewart (2006) developed ground motion amplification relationships using a bedrock shear-wave velocity of 1,000 *m/s* which is consistent to shear-wave velocity of western United States. Figure 2-4 illustrates the shear-wave soil profile for Uplands and Lowlands.

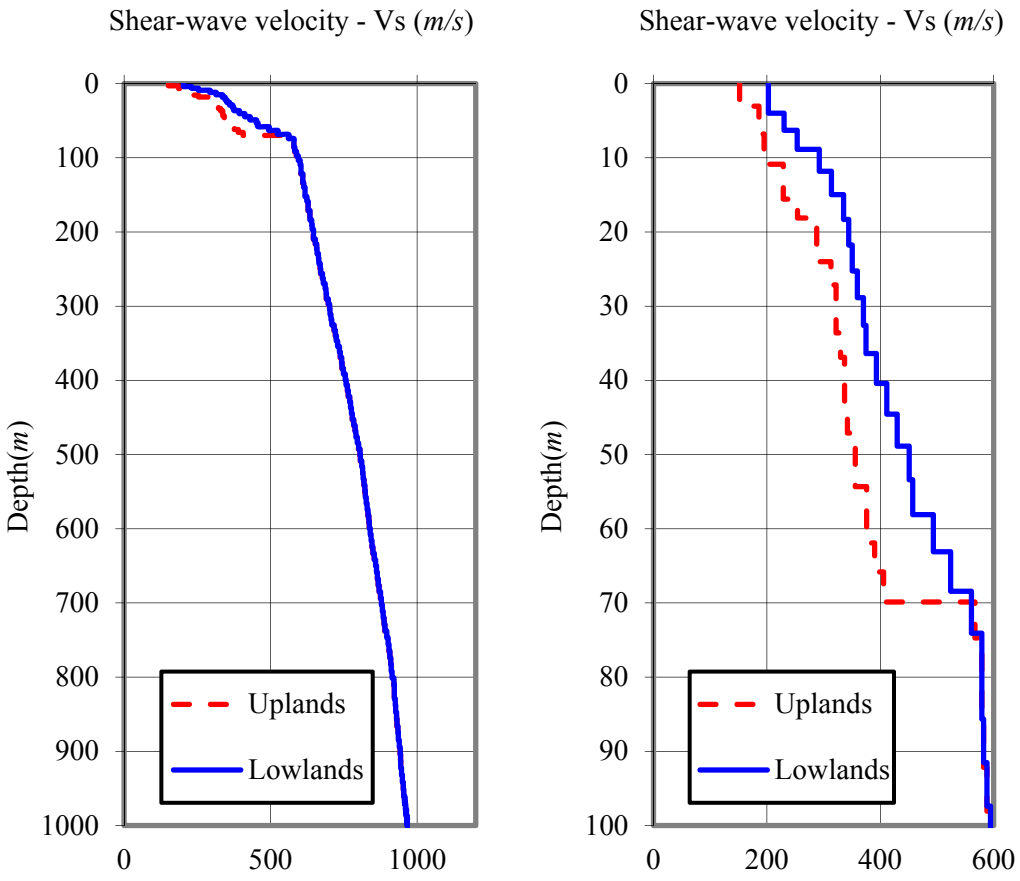

Figure 2-4. Uplands and Lowlands shear-wave velocity soil profile developed by Romero and Rix (2001).

2.7 Variability in Soil's Shear-Wave Profile

Using the EPRI (1993) soil profile database, Toro (1993) developed a probabilistic characterization of soil shear-wave velocity profile and used the resulting probabilistic model to simulate shear-wave profiles. His probabilistic model consists of two separate components, one for the thickness of each layer called the layering model that captures the variability in the thickness of soil layers; and one for the shear-wave velocity associated with each layer called the velocity model to account for the variability in shear-wave velocity of each layer. Based on the data from EPRI (1993) a non-

homogenous Poisson model is used with depth-dependent rate to account for the fact that soil thickness of layers increase with depth. Toro (1993) proposed a modified power law to characterize the depth dependent rate of layer thickness:

$$\lambda(h) = c_3[h + c_1]^{-c_2} \tag{2}$$

where $\lambda(h)$ is the rate of layer boundaries (foot^{-1}) at depth h and coefficients c_1, c_2, and c_3 are estimated from the data. Using the maximum likelihood method, coefficients c_1, c_2, and c_3 are evaluated to be 112, -1.03, and 4.86, respectively (Toro 1993).

The velocity model is defined from a lognormal probability distribution of velocities. Correlation between two layers is defined by the serial auto-correlation factor, ρ, and is presented in the following format (Toro 1993):

$$z_1 = \varepsilon_1 \tag{3-a}$$

$$z_i = \rho z_{i-1} + \sqrt{1-\rho^2}\,\varepsilon_i \tag{3-b}$$

where ε_i is an independent normal variable with zero mean and unit standard variation:

$$z_i = \frac{\ln(v_i) - \ln[v_{median}(h_i)]}{\sigma_{\ln v}} \tag{4}$$

where ρ and $\sigma_{\ln v}$ are estimated to be 0.577 and 0.39 using a linear regression, respectively.

In this study, the variability in soil thickness and the shear-wave velocity is taken into account through the model developed by Toro (1993), which generates a desired number of soil profiles around the base soil profile with a desired probability distribution.

This model statistically captures the soil layer shear-wave velocity and thickness uncertainties and their correlation with depth.

Extreme values of shear-wave velocities are rejected by using the truncated distribution model of ε_i at 2 standard deviations. The coefficient of variation (COV) of 0.15 is used for both thickness and shear-wave velocities to generate soil profiles. For each site depth I used two base shear-wave profiles: one for Uplands and one for Lowlands, and each of them are independently used to simulate 60 soil profiles. Using the model described above, soil profiles with V_{s30} ranging from 220 to 800 *m/s* are simulated for the region. Figure 2-5 shows Uplands (top) and Lowlands (bottom) soil profiles used in analysis of 140*m* soil deposit as an example. Generic Uplands and Lowlands profiles are truncated below 140*m* and a half space with V_s = 3,000 *m/s* is used.

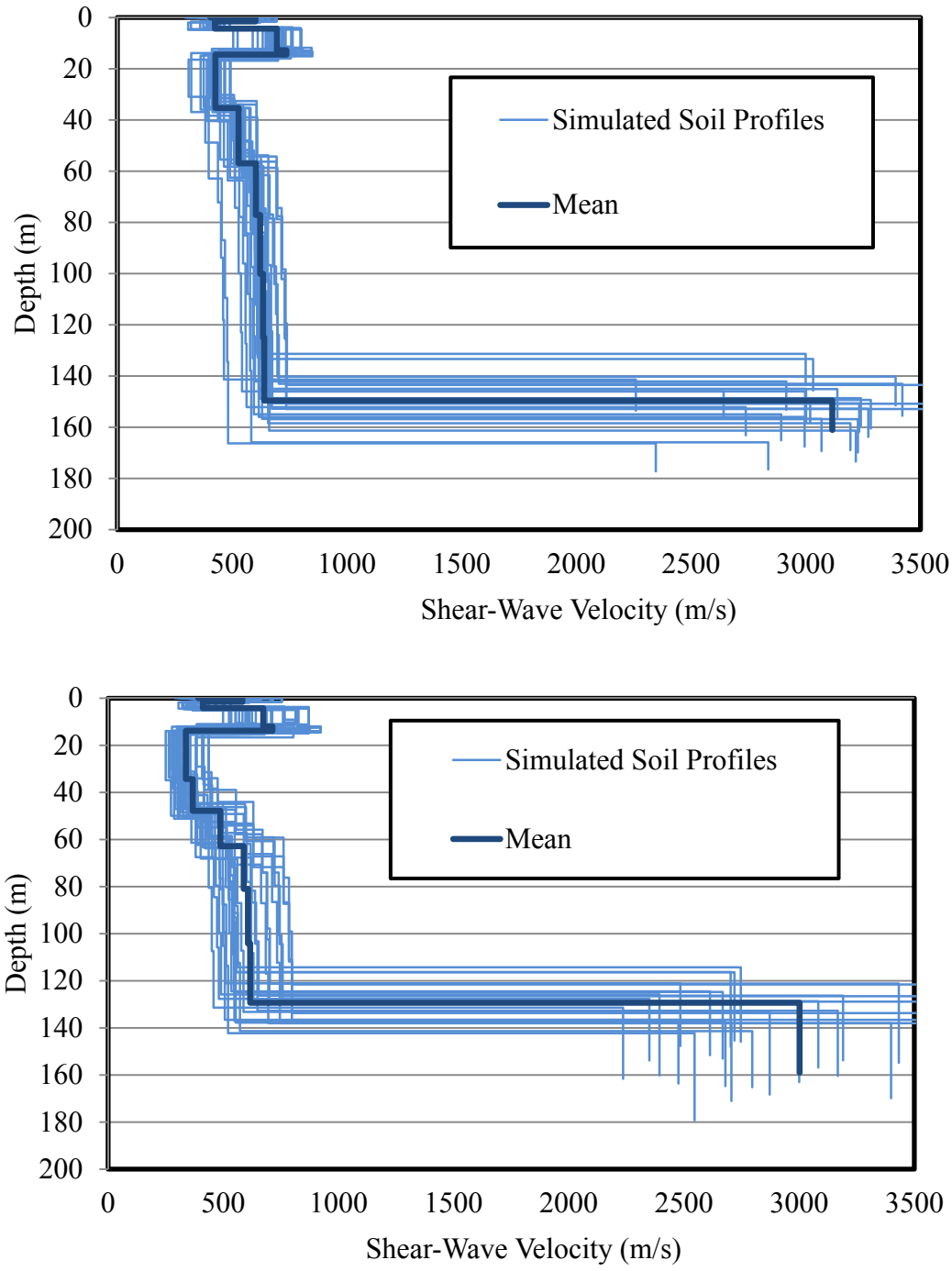

Figure 2-5. 60 Shear-wave velocity profiles simulated for Uplands (top) and Lowlands (bottom) using the Toro (1993) model.

2.8 Proposed Model

Using empirical data, Choi and Stewart (2005) developed the following nonlinear site amplification model as a function of 30*m* shear-wave velocity and *PGA*:

$$\ln(Amp) = a\ln\left(\frac{V_{30}}{V_{ref}}\right) + b\ln\left(\frac{PGA}{0.1}\right) \tag{5}$$

where V_{ref} is the reference shear-wave velocity and parameters *a* and *b* are estimated from the regression analysis. Unlike the model proposed by Boore et al. (1997) and Abrahamson and Silva (1997), equation (5) considers the effects of both *PGA* and V_{s30} on the soil response.

Later, as part of the NGA project, Walling et al. (2008) proposed the following model for the site amplification of ground motions:

For $Vs_{30} < V_{Lin}$

$$\ln(Amp) = a\ln\left(\frac{Vs_{30}}{V_{Lin}}\right) - b\ln\left(PGA_{rock} + c_1\right) + b\ln\left[PGA_{rock} + c_1\left(\frac{Vs_{30}}{V_{Lin}}\right)^n\right] + d \tag{6a}$$

and for $Vs_{30} \geq V_{Lin}$

$$\ln(Amp) = \left(a + bn\right)\ln\left(\frac{Vs_{30}}{V_{Lin}}\right) \tag{6b}$$

where PGA_{rock} is the value of estimated peak ground acceleration at the bedrock, V_{Lin} is the shear-wave velocity above which the site response is linear, and V_{s30} is the shear-wave velocity of the site. The parameters *b* and V_{Lin} are the period dependent parameters and *a*, c_1, and *n* are computed through regression analyses. Walling et al. (2008) set up their model in a way to capture the nonlinearity of the ground motion amplification associated with large values of *PGA* or small values of V_{s30}.

For the Mississippi embayment I propose the following model so that reliable regional earthquake ground motion amplification factors can be determined:

$$\ln(Amp) = f_{base} + f_{depth} + f_{geology} + \eta \tag{7}$$

where f_{base}, f_{depth}, and $f_{geology}$ are the functional forms for base, depth, and geology model, respectively, and η is the residual. The proposed model for estimating site response in the Mississippi embayment is formulated to capture site effects not only due to the soil nonlinearity and effects of ground motion but also the unique characteristic of the study area such as varying soil thickness and two geologic structures. The functional models f_{base}, f_{depth}, and $f_{geology}$ are described next.

2.8.1 Base Functional Model

The base functional form that I used in this study is similar to the model used by Walling et al. (2008):

$$f_{base} = a_1 \ln\left[\frac{V_{S30}}{a_2}\right] - a_3 \ln\left(PGA_{rock} + a_4\right) + a_3 \ln\left[PGA_{rock} + a_4\left(\frac{V_{S30}}{a_2}\right)^{a_5}\right] \tag{8}$$

where a_1 through a_5 are the regression coefficients. Equation (8) is based on the assumption that in the linear range, the base functional form will reduce to the form:

$$f_{base} = a \ln\left[\frac{V_{S30}}{b}\right] \tag{9}$$

which is developed by Boore et al. (1997). In other words, as *PGA* decreases or as V_{s30} increases, the amplification of the ground motion becomes proportional to the V_{s30}. The proposed functional form for the base model also results in the prediction of amplification that is dependent on the V_{s30} at a given *PGA* level.

2.8.2 *Depth Functional Model*

One of the main features of the Mississippi embayment is the variation of thickness of soil deposit on the bedrock throughout the embayment (see Figure 2-2). Using the soil depth model, f_{depth}, in addition to the base model, enables the proposed model to distinguish between sites with different soil thicknesses above the bedrock and to better predict the site amplification due to deep soil deposits:

$$f_{depth} = a_6 \ln\left[\frac{Z_{3000}+a_7}{\exp\left[a_8+\ln\left(\frac{V_{S30}}{a_9}\right)\right]}\right] + a_{10}\ln(PGA_{rock})\times\left|\ln(Z_{3000})-a_{11}\right| + a_{12}\times V_{S30}\times\left|\ln(Z_{3000})-a_{11}\right| \quad (10)$$

In equation (10) Z_{3000} is the depth to the layer with $V_s = 3{,}000\ m/s$ which is assumed to be the shear-wave velocity of the bedrock for the Central United States.

2.8.3 *Geology Functional Model*

As discussed earlier, the geology of the Mississippi embayment can be divided into Lowlands and Uplands. The Lowlands geologic structure in comparison with Uplands tends to show more nonlinear behavior, especially at lower values of V_{s30} and large values of *PGA*. To be able to get a more accurate site amplification factor, I divided the Mississippi embayment into two different geology and introduced the following functional form for $f_{geology}$:

$$f_{geology} = \begin{cases} \dfrac{a_{14}\times\ln(PGA_{rock})++a_{13}}{\ln(Z_{3000})} & \textit{for Uplands} \\ 0 & \textit{for Lowlands} \end{cases} \quad (11)$$

Coefficients a_1 through a_{14} are estimated using the least square method at four spectral periods of *PGA*, 0.2, 1.0, and 5.0 seconds, respectively (see Table 2-3). For each spectral period, the regression coefficients of the model are calculated independent of other periods with the associated analytical data determined from nonlinear analyses at that period.

The sufficiency of the proposed model is investigated by plotting residuals (η in equation 7) against V_{s30}, depth to bedrock, and *PGA* for spectral period of 0.2 and 5.0 seconds in Figure 2-6. From Figure 2-6, one can observe that there is no apparent trend in model residuals vs. different input parameters.

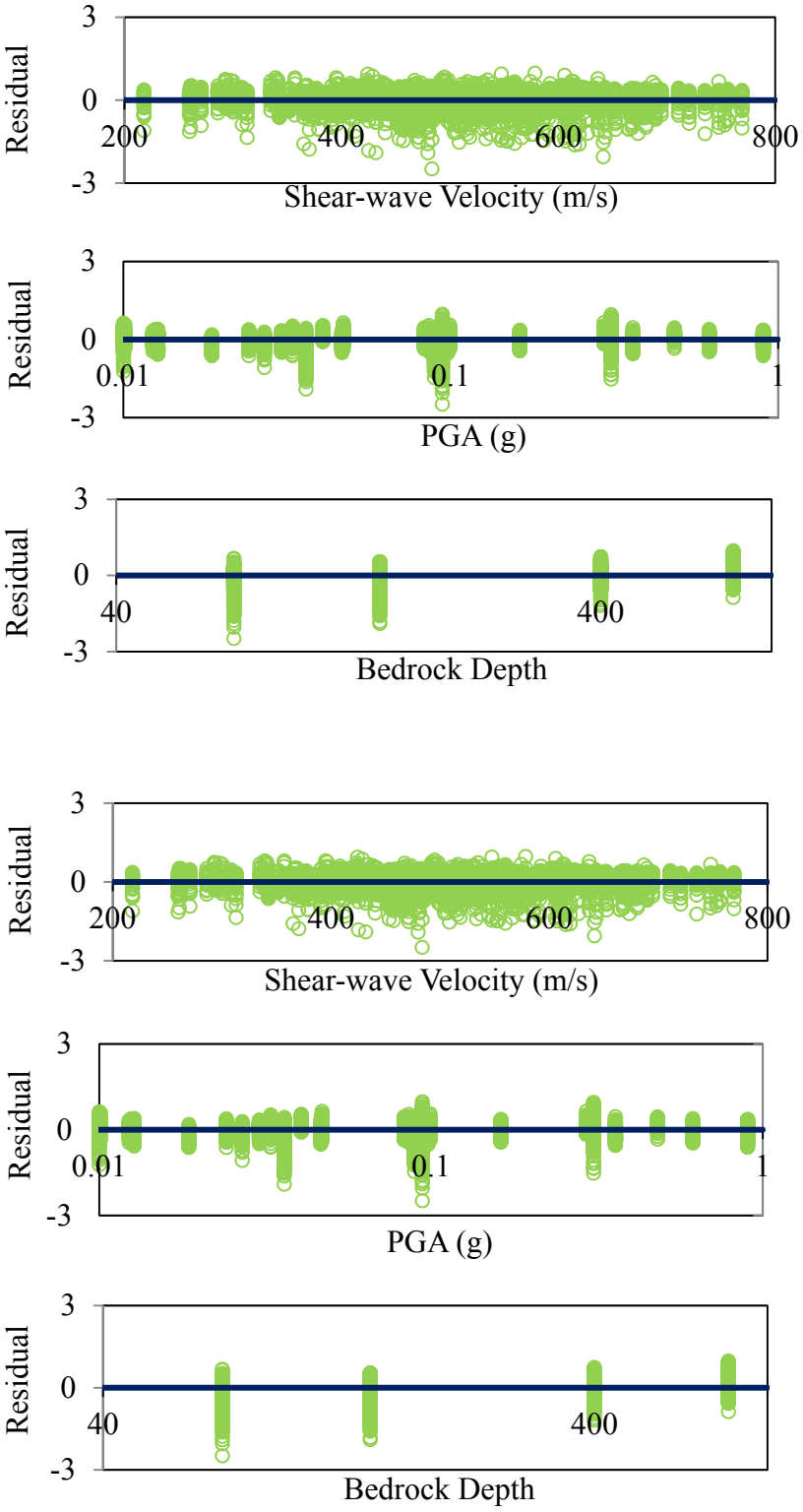

Figure 2-6. Residuals for spectral periods of 0.2 (top) and 5.0 seconds (bottom).

Similar results for residuals are obtained for the regression analysis at *PGA* and 1.0 second. The proposed model seems to provide predicted median amplification factors for each category with reasonable consistency.

2.9 Comparison to Other Studies

Results of this study are compared with Choi and Stewart (2005), Walling et al. (2008), and the NEHRP coefficients, and results are presented in Figures 2-7 through 2-10. Choi and Stewart (2005) defined amplification as the residuals between the spectral acceleration from recordings and what is predicted by ground motion prediction equations. Abrahamson and Silva (1997), Sadigh et al. (1997), and Campbell and Bozorgnia (2003) models are used as the reference, and site factors are developed for each model. Choi and Stewart (2005) site factors are evaluated using coefficients developed for the Abrahamson and Silva (1997) attenuation model.

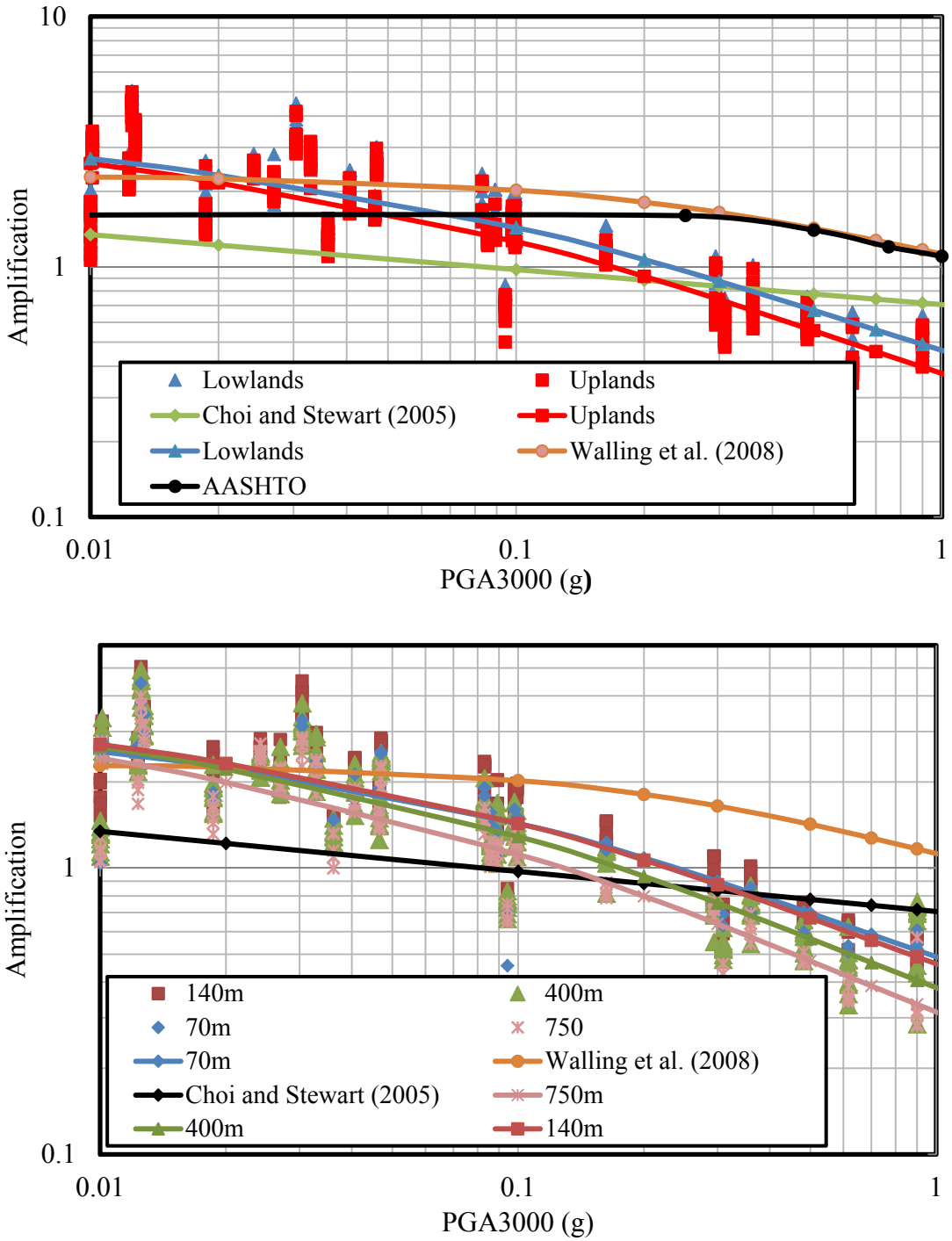

Figure 2-7. Analytical data for Uplands, Lowlands, and associated parametric estimates of ground motion amplification (top) and analytical data for depths 70, 140, 400, 750*m*, and associated parametric estimates of ground motion amplification (bottom) for spectral period 0.0 (or *PGA*).

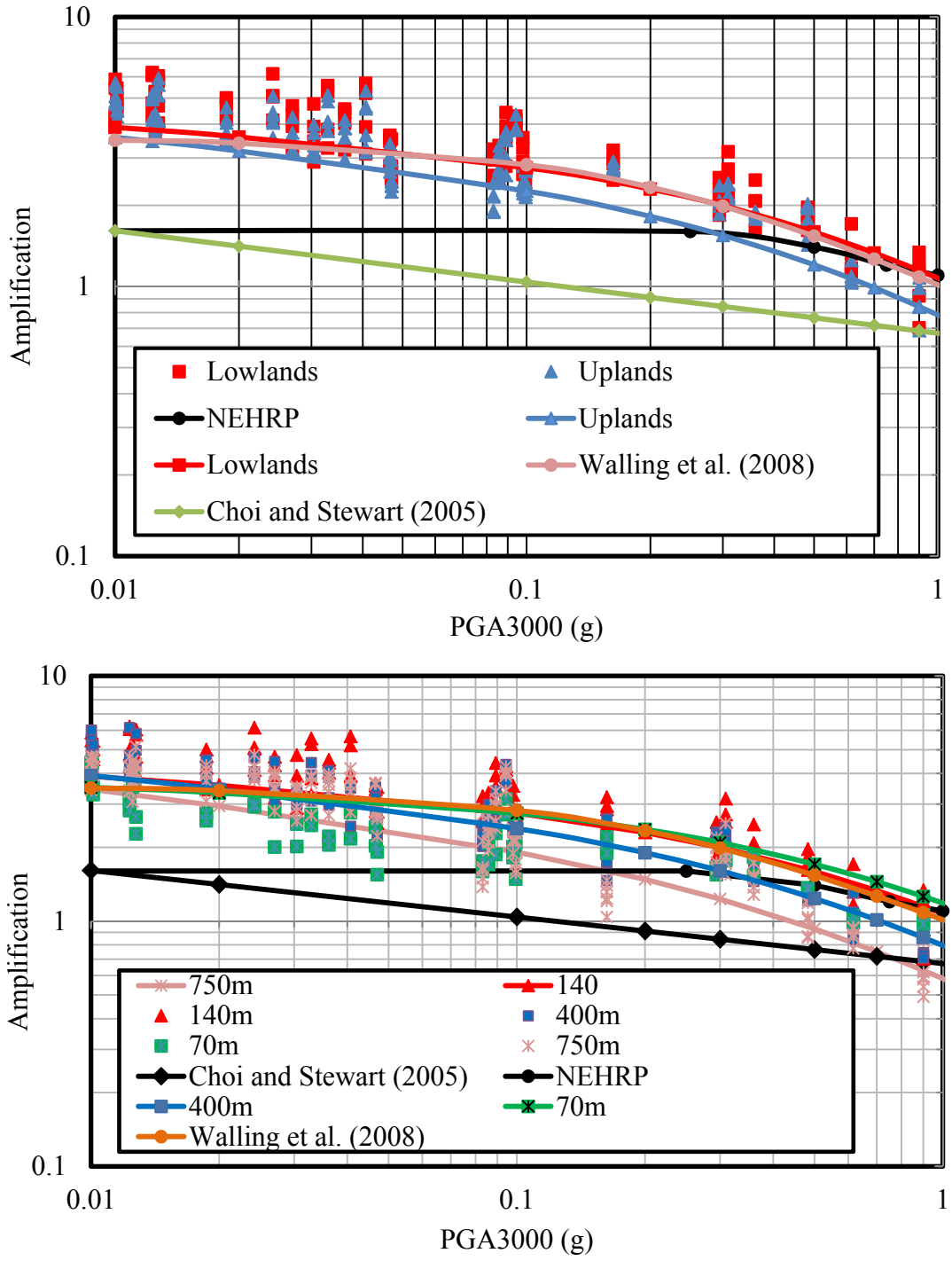

Figure 2-8. Analytical data for Uplands, Lowlands, and associated parametric estimates of ground motion amplification (top) and analytical data for depths 70, 140, 400, 750*m*, and associated parametric estimates of ground motion amplification (bottom) for spectral period 0.2 second.

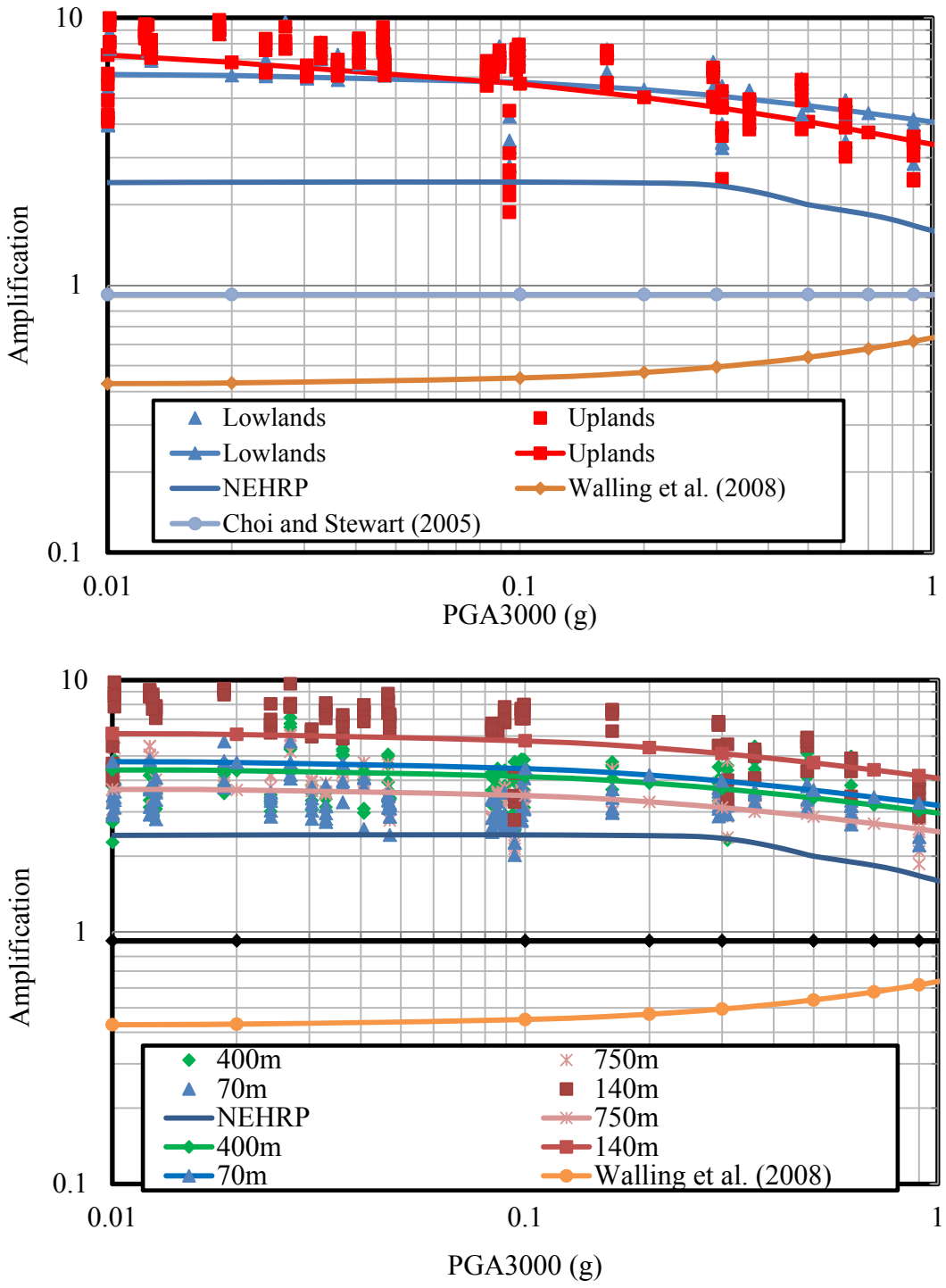

Figure 2-9. Analytical data for Uplands, Lowlands, and associated parametric estimates of ground motion amplification (top) and analytical data for depths 70, 140, 400, 750*m*, and associated parametric estimates of ground motion amplification (bottom) for spectral period 1.0 second.

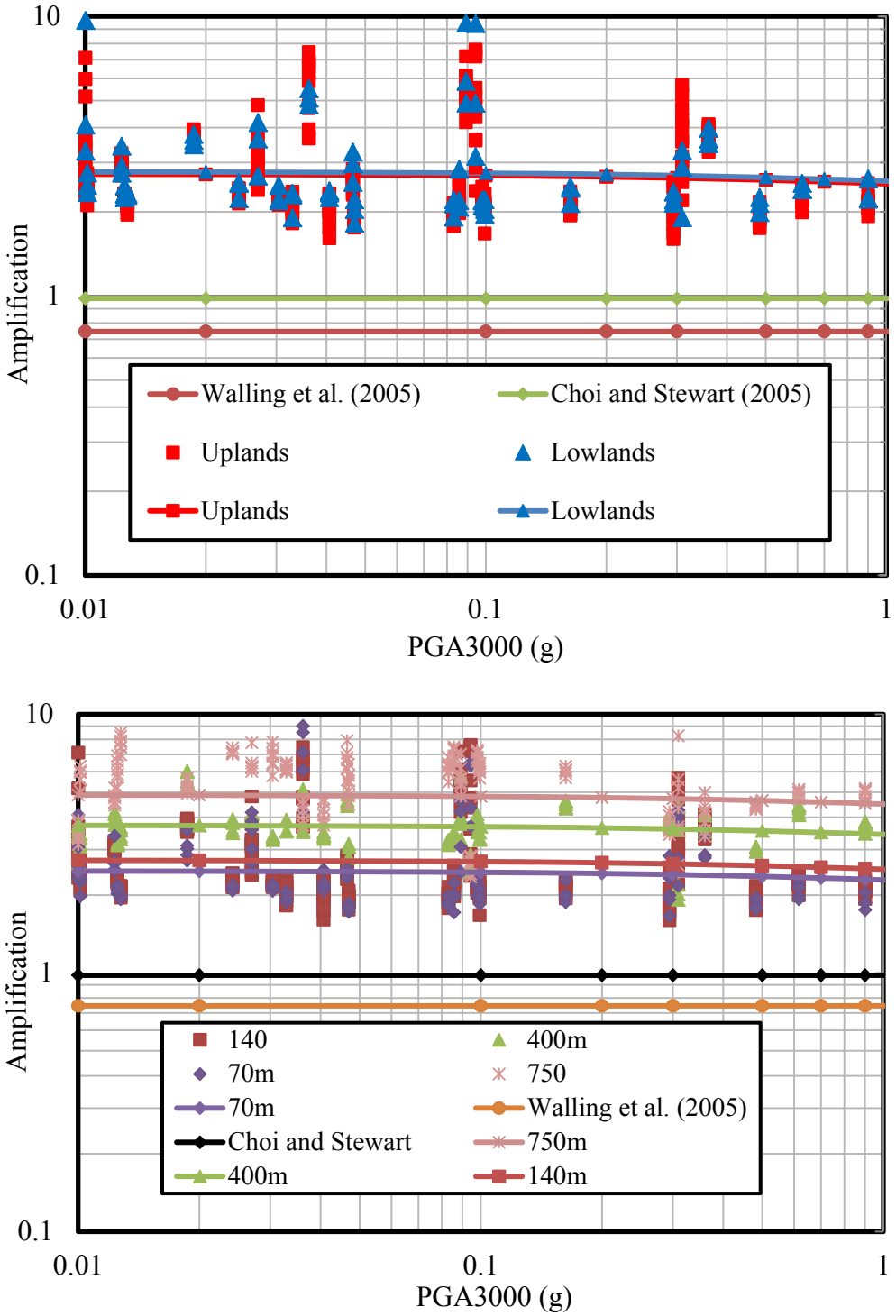

Figure 2-10. Analytical data for Uplands, Lowlands, and associated parametric estimates of ground motion amplification (top) and analytical data for depths 70, 140, 400, 750*m*, and associated parametric estimates of ground motion amplification (bottom) for spectral period 5.0 second.

Figure 2-7 (top) illustrates the amplification versus the bedrock *PGA* for spectral period of *T=0* or *PGA* for Uplands and Lowlands geologic structure. Since Lowlands geologic structure has lower generic shear-wave velocity, sites located within the Lowlands geology have higher amplification factors than sites located within the Uplands geology. The analytical data provided in Figure 2-7 are for shear-wave velocities ranging from 420 to 480 *m/s* with a median value of 450 *m/s*. Figure 2-7 (bottom) illustrates the effect of sediment depth on the site amplification. It can be observed that as the depth of the sediment increases from 70 to 750*m*, the site amplification decreases. This effect becomes more pronounced as the *PGA* of the ground motion at the bedrock increases.

The difference between models developed by Choi and Stewart (2005), and Walling et al. (2008) can be related to the differences in seismological differences and site properties identified in the Mississippi embayment. Similar types of information are shown in Figures 2-8 through 2-10. It is important to know that for high spectral periods (low spectral frequencies), such as 5 seconds (0.2 Hz), as the sediment thickness increases, the site amplification increases. This is in the reverse order as for low spectral periods (high spectral frequencies). Furthermore, as it can be observed from Figure 2-10, the site amplification seems to remain almost constant; there is small decrease with the increase in peak ground acceleration at the reference rock for all sediment depths. Another trend observed in Figures 2-7 through 2-10 is the reduction of effect of the geology in ground motion amplification with the increase of spectral period. At longer spectral periods, geology plays a small role in ground motion amplification, and site response in the Mississippi embayment becomes independent of the geology. Furthermore, since the only difference in the Uplands and Lowlands shear-wave velocity

is on the top 70*m*, the effect of geology decreases when the depth of the bedrock increases.

2.10 Conclusions

In this research I developed a parametric site response model for the Mississippi embayment as a function of *PGA* on the reference bedrock, V_{s30}, depth of soil columns, and geology using the nonlinear site response analyses. Using seismological parameters of the study area, I simulated a series of input ground motions. The input ground motions are then propagated through different soil profiles. Soil profiles are varied using the Toro (1993) model in a way to capture the uncertainty associated with shear-wave velocity and thickness. Four different bedrock depths are also used in evaluating site response analyses. Considering all the input cases, more than 12,000 nonlinear runs are conducted.

The results of the analytical analyses are used to fit a model to predict the ground motion site amplification in the region. The proposed model consists of three different functional forms, to take into account the unique features of the study area such as variable bedrock depth and having two dominant geological structures.

The proposed model is used to compare the site response of the Mississippi embayment with other models developed for other study areas. Results from this study show that the site amplification within the Mississippi embayment is relatively higher, especially at low periods and low *PGA*s, in comparison with the proposed values of NEHRP, Choi Stewart (2005), and Walling et al. (2008), which are derived with data from the west coast. Geology also has a considerable role in the site response of the study area when the bedrock depth is relatively shallow. The effect of geology decreases as the depth of the bedrock increases.

Study of the ground motion site amplification within the Mississippi embayment indicates more nonlinearity in short periods in comparison with the same type of studies which have been focused on data from other regions. In other words, for short periods at low values of *PGA*, estimated values of the ground motion amplification for the Mississippi embayment tends to be higher relative to values proposed by NEHRP, Choi Stewart (2005), and Walling et al. (2008). For ground motions with high *PGAs*, the proposed model predicts smaller site amplification.

For long periods, the Mississippi embayment shows no nonlinearity in the ground motion amplification, which is consistent with findings of other studies (Choi Stewart 2005, Walling et al. 2008, and NEHRP); but the predicted value of ground motion amplification is substantially higher in comparison with values of NEHRP, Choi Stewart (2005), and Walling et al. (2008).

Table 2-3. Coefficients a_1 to a_{14} of the site response model

Period	*Base Model*					*Depth Model*						*Geology Model*		
(sec)	*a1*	*a2*	*a3*	*a4*	*a5*	*a6*	*a7*	*a8*	*a9*	*a10*	*a11*	*a12*	*a13*	*a14*
PGA	*1.382*	*1897*	*-0.686*	*1.901*	*1.6176*	*-0.652*	*517*	*8.78*	*96.1*	*-0.03585*	*0.014*	*0.00005*	*-1.05298*	*-0.18068*
0.2	*2.629*	*1651*	*-2.035*	*3.500*	*0.8387*	*-1.271*	*900*	*10.09*	*100.4*	*-0.06325*	*3.341*	*-0.00004*	*-1.55272*	*-0.24581*
1	*1.804*	*893*	*-2.607*	*1.221*	*0.8176*	*0.200*	*878*	*-0.79*	*281.1*	*0.00275*	*4.933*	*-0.00058*	*-0.95441*	*-0.38725*
5	*0.970*	*632*	*-2.821*	*1.893*	*0.5614*	*0.751*	*162*	*5.81*	*83.8*	*-0.00019*	*2.118*	*-0.00027*	*0.10866*	*0.00435*

2.11 References

Atkinson, G. M., and Boore, D. M. (2006). "Earthquake ground-motion prediction equations for eastern North America." *Bulletin of the Seismological Society of America,* 96, 2181–2205.

Assimaki, D., and Li, W. (2012). "Site- and ground motion-dependent nonlinear effects in seismological model predictions." *Soil Dynamics and Earthquake Engineering,* 32 143–151.

Bicker, A. R. (1969). Geologic Map of Mississippi. *Mississippi Geologic Survey*, scale 1:500000.

Bonilla, L. F., Lavallée, D., and Archuleta, R. J. (1998). "Nonlinear site response: laboratory modeling as a constraint for modeling accelerograms. In: Irikura." K., Kudo, K., Okada, H., Sasatani, T. (Eds.), *Proceedings of the Second International Symposium on the Effects of Surface Geology on Seismic Motion* 2, A. A. Balkema, Brookfield, VT, 793–800.

Bonilla, L. F. (2000). "Computation of linear and nonlinear site response for near field ground motion." *Ph.D. Dissertation. University of California*, Santa Barbara, 285.

Boore, D. M. Joyner, W. B., and Fumal, T. E., (1997). "Equations for estimating horizontal response spectra and peak acceleration from western North American earthquakes: A summary of recent work." *Seismological Research Letters,* 68, 128–153.

Borcherdt, R. D. (2002a). "Empirical evidence for acceleration-dependent amplification factors." *Bulletin of the Seismological Society of America,* 92, 761–782.

Borcherdt, R. D. (2002b). "Empirical evidence for site coefficients in building code provisions." *Earthquake Spectra,* 18 (2), 189–217.

Bresne, I. A., and Wen, K. L. (1996). "Nonlinear Site Response – A Reality?" *Bulletin of the Seismological Society of America,* 86, 1964-1978.

Building Seismic Safety Council (BSSC) (2001). "NEHRP Recommended Provisions for Seismic Regulations for New Buildings and Other Structures, Part 1: Provisions and Part 2: Commentary, Federal Emergency Management Agency." FEMA-368 and FEMA-369, Washington D.C., February.

Campbell, K. W., and Bozorgnia, Y. (2008). "NGA ground motion model for the geometric mean horizontal component of *PGA*, PGV, PGD and 5% damped linear elastic response spectra for periods ranging from 0.01 to 10 s." *Earthquake Spectra,* 24, 139–171.

Choi, Y., and Stewart, J. P. (2005). "Nonlinear Site Amplification as Function of 30m Shear Wave Velocity." *Earthquake Spectra* 21, 1–30.

Cramer, C. H., Boyd O. S. (2012). "Why the New Madrid Earthquakes are M7–8 and the Charleston Earthquake is ~M7." submitted to *Bulletin of the Seismological Society of America*

Cramer, C. H. (2006). "Quantifying the uncertainty in site amplification modeling and its effects on site-specific seismic-hazard estimation in the upper Mississippi embayment and adjacent areas." *Bulletin of the Seismological Society of America,* 96, S2008–S2020.

Dobry, R., Borcherdt, R. D., Crouse, C. B., Idriss, I. M., Joyner, W. B., Martin, G. R., Power, M. S., Rinne, E. E., and Seed, R. B. (2000). "New site coefficients and site classification system used in recent building seismic code provisions." *Earthquake Spectra,* 16 (1), 41–67.

Electric Power Research Institute (EPRI) (1993). "Guidelines for Determining Design Basis Ground Motions. Palo Alto, CA." *Electric Power Research Institute,* 1–5 EPRI TR-102293.

Field, E. H. (2000). "A modified ground motion attenuation relationship for southern California that accounts for detailed site classification and a basin depth effect." *Bulletin of the Seismological Society of America* 90, S209–S221.

Hanks, T. C., and McGuire, R. K. (1981). "The character of high-frequency strong ground motion." *Bulletin of the Seismological Society of America,* 71, 2071–2095.

Hartzell, S., Bonilla, L. F., and Williams, R. A. (2004). "Prediction of nonlinear soil effects." *Bulletin of the Seismological Society of America,* 94, 1609–1629.

Kramer, S. L., (1996). "Geotechnical Earthquake Engineering." Prentice Hall, New Jersey, 653 pp.

Leon, J. A. F. (2007). "Numerical Simulation of earthquake ground motions in the upper Mississippi embayment." *Ph.D. Dissertation. Georgia Institute of Technology*, Atlanta, p. 365.

Li, X., and Liao, Z. (1993). "Dynamic skeleton curve of soil stress-strain relation under cyclic loading earthquake." research in China 7, 469 – 477.

McGuire, R. K., Becker, A. M., and Donovan, N. C. (1984). "Spectral estimates of seismic shear waves." *Bulletin of the Seismological Society of America,* 74, 1427–1440.

Miller, R. A., Hardeman, W. D., Fullerton, D. S. (1996). "Geologic map of Tennessee. West Sheet." *State of Tennessee, Department of Conservation, Division of Geology* Scale 1:250,000.

Park, D., and Hashash, Y. M. A. (2005). "Evaluation of seismic site factors in the Mississippi embayment. II. Probabilistic seismic hazard analysis with nonlinear site effects." *Soil Dynamic Earthquake Engineering,* 25, 145–156.

Romero, S., and Rix, G. J. (2001). "Regional variations in near surface shear-wave velocity in the Greater Memphis area." *Engineering Geology,* 62, 137–158.

Romero, S., and Rix, G. J. (2005). "Ground motion amplification of soils in the upper Mississippi embayment." *National Science Foundation Mid America Earthquake* Center, Report No. GIT-CEE/GEO-01-1.

Silva, W. J., Abrahamson, N., Toro, G., and Costantino, C. (1997). "Description and validation of the stochastic ground motion model.' *Report submitted to Brookhaven National Laboratory*, Associated Universities, Inc. Upton, New York 11971, Contract No. 770573.

Silva, W. J., Li, S., Darragh, R. B., and Gregor, N. (1999). "Surface geology based strong motion amplification factors for the San Francisco Bay and Los Angeles areas." *Report to Pacific Earthquake Engineering Research Center*, Richmond, California.

Stewart, J. P., Liu, A. H., and Choi, Y. (2003). "Amplification factors for spectral acceleration in tectonically active regions." *Bulletin of the Seismological Society of America,* 93, 332–352.

Stewart, J. P., and Kwok, A. O. (2008). "Evaluation of the effectiveness of theoretical 1D amplification factors for earthquake ground-motion prediction." *Bulletin of the Seismological Society of America* 96, 1422–1436.

Toro, G. R., (1993). "Probabilistic model of soil-profile variability, in Early Site Permit Demonstration Program: Guidelines for Determining Design Basis Ground Motions, J. F. Schneider (Editor)." *EPRI Project RP3302* II, Appendix 6A, Electric Power Research Institute.

Toro, G. R., and McGuire, R. K. (1987). "An investigation into earthquake ground motion characteristics in eastern North America." *Bulletin of the Seismological Society of America,* **77**, 468–489.

Toro, G. R., and Silva, W. J., (2001). "Scenario earthquakes for Saint Louis, MO, and Memphis, TN, and seismic hazard maps for the central United States region including the effect of site conditions." *Final technical report to the USGS*, 10 January 2001, Risk Engineering, Inc., Boulder, Colorado.

Towhata, I., and Ishihara, K. (1985). "Modeling soil behavior under principal axes rotation." *Fifth International Conference on Numerical Methods in Geomechanics*, Nagoya, 523–530.

Van Arsdale, R. B., and Ten Brink, R. K. (2000). "Late cretaceous and cenozoic geology of the New Madrid seismic zone." *Bulletin of the Seismological Society of America* 90, 345–356.

Vucetic, M. (1990). "Normalized behavior of clay under irregular cyclic loading." *can. Geothech.* J., 27, 29–46.

Walling, M., Silva, W. J., and Abrahamson, N. A. (2008). "Nonlinear site amplification factors for constraining the NGA models." *Earthquake Spectra,* 24, 243–255.

Wen, Y. K., and Wu, C. L. (1999). "Generation of ground motions for mid-America cities." *Mid-American Earthquake Center Report*.

3 Capturing Uncertainty in Ground Motion Selection and Scaling

3.1 Introduction

Time-history analysis may be required when the nonlinear performance of a structure needs to be addressed. Instances that require time-history analysis include very tall buildings or long bridges, complex buildings with extreme mass and/or geometric irregularities, structures with base isolation or supplementary damping devices, structures designed for high ductility demand, and particularly critical structures for which any damage has potentially far-reaching consequences in terms of safety. A number of GMs are needed to be used as the input of time-history analysis. These GMs must represent the main seismological parameters and geologic features of the study site. Selected acceleration time-histories must have specific response spectrum values at some specific spectral periods. These specific values are called target spectrum and are dependent on the spectral period and the shear-wave velocity profile of the site. In the time-history analysis procedures, the variability in selected GMs will be transferred to the structural response of interest, and make it difficult for the engineer to make a reliable estimate of the response of the structure. In the present research, I include the epistemic uncertainties associated with different seismic hazard scenarios in the variability of response of the structure through the GM selection procedures.

Different seismic codes have different GM selection provisions. AASHTO (2004) requires *"at least three response-spectrum compatible time histories shall be used for representing the design earthquake (ground motions having seven present probability of exceedance in 75 years) when conducting dynamic ground motion response analyses or nonlinear inelastic modeling of bridges."* It also adds *"if a minimum of seven time*

histories is used for each component of motion, the design actions may be taken as the mean response calculated for each principal direction." AASHTO (2003) also sets up the procedure to obtain target response spectrum (Article 3.4.3.1.)

FEMA 450 (2003) provides guidelines in selecting earthquakes in Section 5.4: *"A suite of not fewer than three appropriate ground motions shall be used in the analysis."* But, in Section 5.4 of the commentary it states: *"As a minimum, the Provisions require that suites of ground motions include at least three different records. However, suites containing larger number of records are preferable, since when more records are run, it is more likely that the differing response possibilities for different ground motion characteristics are observed. In order to encourage the use of larger suites; the Provisions require that when a suite contains fewer than seven records, the maximum values of the predicted response parameters be used as the design values. When seven or more records are used, then mean values of the response parameters may be used."*

Iervolino and Cornell (2005) discussed the question *"What earthquake parameters do we have to try to match when selecting the records?"* They statistically studied the effect of the GM selection and scaling parameters such as the magnitude and the distance on the nonlinear seismic response of structures through hypothesis testing. They selected earthquakes from two different categories: one was carefully chosen to represent a specific magnitude and source to site distance scenario, and the other class of GMs were chosen randomly from the database of real GMs. Several structural models belonging to both single degree of freedom and multi-degree of freedom are used in the structural time-history analysis and are chosen to represent different structural systems. Their statistical analysis revealed that the principal seismological parameters such as

magnitude, distance, and scaling do not affect the nonlinear response of structures. They also concluded that concern about scenario-to-scenario record scaling may not be justified.

Bommer and Acevedo (2004) studied different procedures and influential parameters of the GM selection from a real database. They illustrated the application of both geophysical and response spectral search criteria using compatible scenarios. The selected records were analyzed and adjusted to produce suites of time-histories suitable for dynamic analysis. They presented some recommendations for the selection and using real GMs based on the GM's seismological parameters such as the magnitude, the source to site distance, and the site classification. They also addressed the spectral matching and discussed concerns in using the spectral matching procedure. Naeim et al. (2004) developed a method to select *"a union of 7 records and corresponding scale factor as a single individual"* from a large database. Unlike the conventional scaling methods where a preset number of GMs are selected first and then scaled to match the target, the proposed method is capable of searching the whole database and selecting a suite of ground motions with response spectra that has minimum alternation with the target. In their method, they used a genetic algorithm to minimize the difference between the target spectrum and average of selected records from a database. They also modified their approach so that the selected records have an average greater than the target in a range of periods.

Goulet et al. (2008) assessed and compared 16 different methods of GM selection and scaling methods for dynamic analysis. Their research was part of the ground motion selection and modification program formed within the Pacific Earthquake Research

(PEER) Center. The goal of the program was to determine which method results in unbiased estimates of structural response parameters. All the ground motion selection and scaling methods are grouped into two main categories: methods based on scaling to a UHRS, and methods that take into account the record properties that affect the nonlinear response of structures.

Lamprey and Abrahamson (2006) discussed a new method in selection of GM time series and scaling limits that reduces the structure's nonlinear response variability. They defined and used a simple structural model as a representative of a more complicated nonlinear model. Using the simple model, they find appropriate time series that have properties that lead to a reduction of variability of the average response of the simple model. Using a simple nonlinear model will enable the user to evaluate a large number of candidate acceleration time series and identify those GMs in the database that lead to a reduction of the average response variability. They also used the simple representative model to study the effects of scaling of GMs on the final response of the structure. Baker and Cornell (2006) questioned the credibility of UHRS as an appropriate target response in their study, claiming that UHRS is constructed by using maximum values of spectral accelerations at all periods and thus is a conservative target for GM selection. They formulated an alternative target response spectra named Conditional Mean Spectrum (CMS) based on the experimental correlation of spectral values at different periods. They also selected GMs based on the number of standard deviation above or below the mean value, known as ε, and argued that this parameter plays an important role in the spectral shape of GMs and thus should be a part of the GM selection criteria.

Jayaram and Baker (2011) argued that the variance of the target is an important parameter in the selection of GM for time-history analysis and should be considered in the selection procedure. The CMS procedure developed by Baker (2011) and Baker and Cornell (2006), which considers the correlation between different periods, was used as the target. The variance of the target is captured through probabilistically generating a number of response spectra from the target's distribution. GMs are selected based on the resemblance of their response spectra to the generated response spectra. A greedy optimization technique was used to improve the match between the target's mean and variance and the selected set of GMs. The greedy optimization technique is an iterative algorithm that improves the mean and variance of the selected suite by replacing each GM in the suite with other GMs in the database until the desired level of match is reached.

As mentioned above, in the time-history analysis of important civil infrastructure, the GM selection is required and there are limited and sometimes contradicting guidelines available for practicing engineers (Katsanos et al. 2010). Therefore, the choice of which GM selection method to use is based on the personal judgment and the experience of the earthquake engineer. The objective of this study is to introduce and to automate a step-by-step procedure to integrate a target's variability originated from epistemic uncertainties in the procedure of the GM selection. The proposed procedure is presented through studying a sample site in the Central United States. I select a set of GMs from the database in a way that the mean of the selected GMs equals the mean of the target spectral acceleration at period(s) of interest; and their variability at different periods equals different possible hazard scenarios. First, I perform a site-specific study for a

selected site in the north of the New Madrid seismic zone (Latitude: 37.7°, Longitude: -89.225°) and generate the UHRS for the site, and then I determine uncertainties at different spectral periods. In this study, I use a logic tree procedure similar to the one used by the United States Geological Survey (USGS) 2008 report (Peterson et al. 2008) to account for different possible scenarios of hazard. I also make some simplifying assumptions on the logic tree branches and associated weights to maintain the PSHA analyses manageable. These simplifying assumptions do not influence the proposed procedure. The Monte Carlo technique is used to simulate a large set of response spectra for a specific hazard level that have the mean and the variability as the target. GMs from three different databases are used as the seed for the GM selection to test the capability of different sources in providing candidate earthquakes. Earthquakes are selected separately from the database of real ground motions and synthetic records produced using the stochastic point-source model and the stochastic finite-fault model.

The proposed GM selection method has four main steps: (1) performing a site-specific study to determine the target response spectrum (UHRS) and obtaining the upper and lower limits of the target using a logic tree; (2) generating a large number of (5,000) individual target response spectra sets using the Monte Carlo simulation technique, and selecting the set of individual target response spectra that best matches the target and its variability; (3) setting GM's selection parameters such as scaling method, scaling limits and dominant scenario (*i.e.,* magnitude, distance, and ε obtained from deagreggation analysis) for the study site; and (4) selecting GMs from the databases. It is important to note that assumptions such as the definition of the logic tree branch, logic tree branch

weights, scaling method, and limits on scaling factors are among decisions that earthquake engineers should make for each project.

3.2 Site-Specific Study

3.2.1 Logic Tree

The epistemic uncertainties are taken into consideration in the PSHA using a logic tree. Each branch of the logic tree represents a possible hazard scenario and receives a relative weight based on its scientific credibility. Since the study site is located in the Central United States, I choose a logic tree that is derived from the USGS update for the Central United States (Peterson et al. 2008). I used the New Madrid hypothetical fault locations defined by the 2008 USGS hazard maps as well as two different ground motion prediction models (Tavakoli and Pezeshk 2005; Campbell 2003) in performing the PSHA. For simplicity I assigned equal weight to all the branches of the logic tree. Figure 3-1 shows the schematic presentation of the logic tree used in this study. The locations of the hypothetical faults considered in the logic tree are shown in Figure 3-2. Sabetta et al. (2005) conducted research on the sensitivity of seismic hazard analyses to the logic tree weights and branches. Their study showed that relative weights of GMs in the logic tree have less influence on the hazard analysis when there are four or more attenuation models used in the logic tree. Discussion about the logic tree and weights assigned to each branch is not the subject of this study and do not affect the procedure of the proposed method.

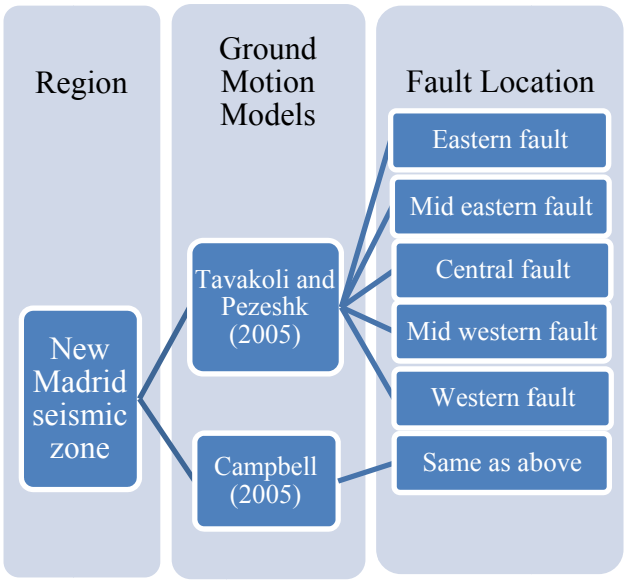

Figure 3-1. Locations of the modeled New Madrid hypothetical faults (Peterson et al. 2008) and the location of site studied.

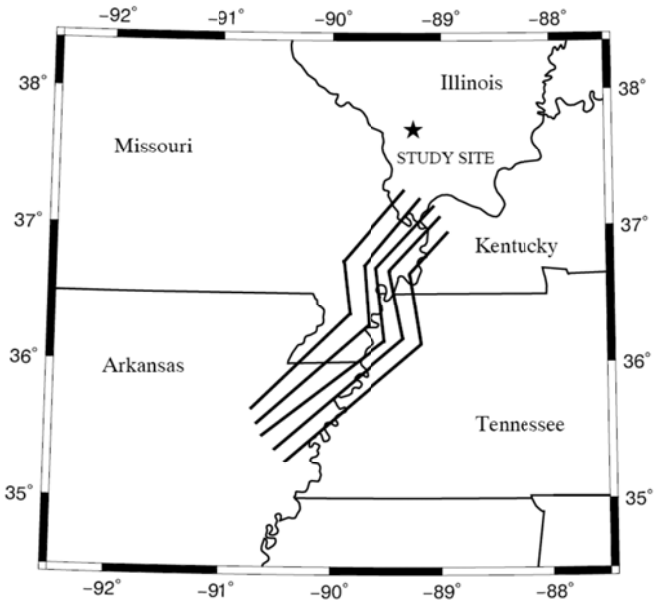

Figure 3-2. Locations of the modeled New Madrid hypothetical faults (Peterson et al. 2008) and the location of site studied.

3.2.2 UHRS, Upper, and Lower Limits

An accepted target spectrum in dynamic design of structures is the UHRS. Although there are some concerns about the UHRS being conservative as a target for dynamic analysis (Baker and Cornell 2006), almost all the seismic codes accept the UHRS as a target for structural seismic design. I decided to be consistent with current seismic codes in the definition of the target. To perform the PSHA, I used the computer program EZ-FRISK (http://www.ez-frisk.com/index.html). For this study I select a site located in the Central United States with Longitude and Latitude of 37.7° and -89.225°, respectively. The PSHA is conducted using each branch of the logic tree separately, and the results are 10 different hazard curves associated with each branch of the logic tree for the return period of 2,475 years (2% probability of exceedance in 50 years). In this study, the average and mean $\pm 1\sigma$ hazard curves will be used to estimate the mean (or UHRS), upper, and lower limits, respectively. Figure 3-3 shows hazard curves for the logic tree defined in this study for spectral periods of 0.01 and 1.00 second for illustration purposes. In Figure 3-3, the mean and mean $\pm 1\sigma$ are the intersection of the horizontal line associated with the 2% probability of exceedance and the mean and mean $\pm 1\sigma$ hazard curves. Using the same procedure for other spectral periods, I generated the UHRS and the upper and the lower limits of the target associated with mean $\pm 1\sigma$ of the hazard curves for the study site. Note that there is no simple relation between SA_{mean}, SA_{upper}, and SA_{lower} for a known probability of exceedance.

In this study, I consider SA_{mean} (UHRS) as the target response spectrum and $SA_{upper} - SA_{lower}$ as the variability band that represents the uncertainties associated for the

study site. Figure 3-4 illustrates the target, the upper, and the lower limits of UHRS for the selected site.

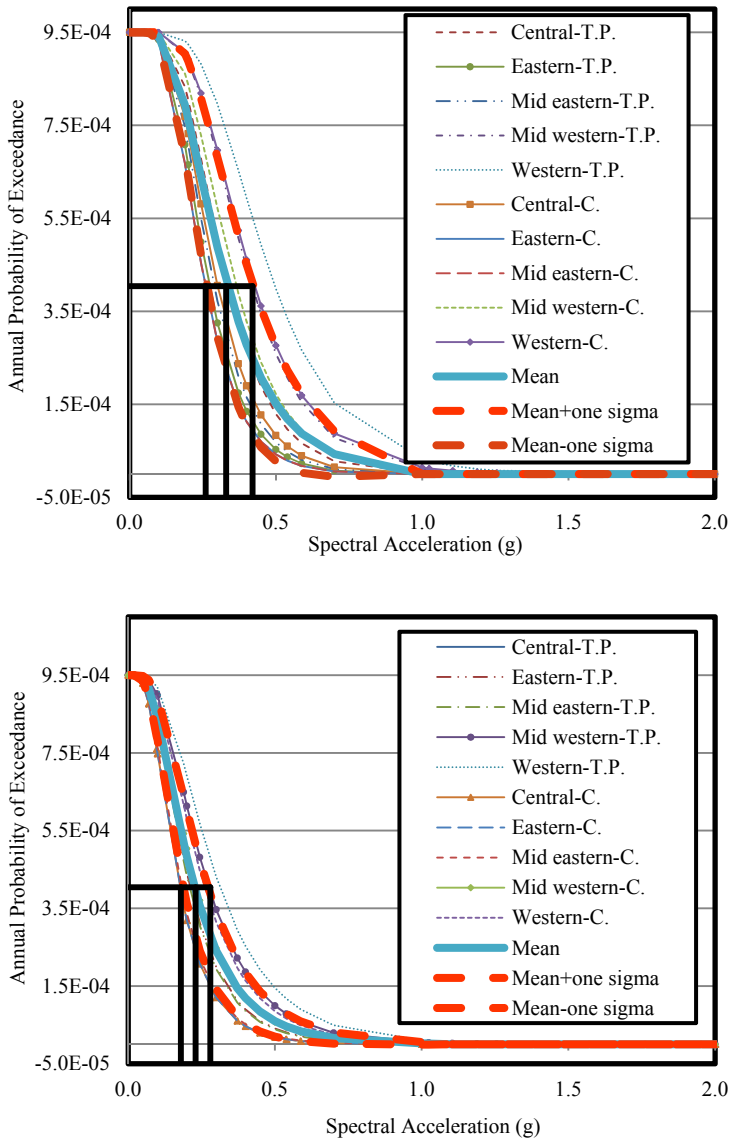

Figure 3-3. Hazard curves for the spectral periods of 0.01 sec (top) and 1.00 sec (bottom). Black horizontal line associates with 2% probability of exceedance and its intersection with the mean, mean $+\sigma$, and mean $-\sigma$ hazard curves marks UHRS, SA_{upper}, and SA_{lower}. [T.P. stands for Tavakoli and Pezeshk (2005) and C. stands for Campbell (2005)].

3.3 Generation and Selection of Individual Target Response Spectrum

The outcome of this step is a set of individual target response spectra which has a mean close to the target and a standard deviation close to the variability of the target at different spectral periods. I modified the method proposed by Jayaram et al. (2011) to generate individual response spectra. The number of response spectra in each set is equal to the number of GMs needed for the design purposes. Jayaram et al. (2011) improved the mean and the variability of the set of individual target spectra by a *"greedy"* procedure. The method proposed in this study can generate a smaller number of response spectra with the same properties as of the target (*i.e.*, mean and variability), and no other improvement of individual target spectra is needed. In the proposed model, I first simulated a set with 7 response spectra, to be consistent with FEMA 450, in a way that the mean of the simulated response spectra is equal to the UHRS and all of the individual spectrum fall within the upper and lower limits. Then I will select 7 GMs from candidate earthquakes that most resemble the 7 simulated individual target response spectra. Now, these 7 individual response spectra become target spectra. In other words, I will have 7 individual target spectra rather than one. Since 7 individual target response spectra have captured the mean and the seismological uncertainties of the study site, the selected GMs will also have the same mean and variability as the target.

3.3.1 Generation of Individual Targets

The distribution of an earthquake's response acceleration around SA_{mean} is assumed to be a lognormal distribution. In this study, the Monte Carlo technique is used to generate a set of 7 lognormally distributed numbers at each spectral period, with a mean of SA_{mean} and a standard deviation which equals the variability of the target at each

spectral period (an array of 7×20). Since 7 is not considered a statistically large number, the mean and standard deviation of generated values at different periods have little chance of being equal to the desired values throughout all spectral periods at the first try. As a result, 5,000 sets of individual target response spectra were generated and the set having the closest mean and standard deviation to SA_{mean} and the target's variability was chosen. Generating 5,000 set (or a large number) would enable us to select an even small number of GMs with the desired mean and variability. As expected, when the number of GMs needed for the time-history analysis of structures increases, fewer sets are needed to reach a certain level of error. It is worth noting that the Monte Carlo technique is very efficient in generating individual targets and the computer time for generation of the individual targets are relatively low.

3.3.2 Selection of the Best Individual Target Set

The selection of the best generated set that corresponds to the individual target response spectrum is based on two different error measurements. The first error measurement is the dissimilarity between the mean of 7 generated response spectra in each set and the target (*i.e.,* SA_{mean}). The second error measurement is the dissimilarity between the variability of the target and the standard deviation of the generated individual response spectrum. The following formulations are used to quantify the error of each set in the selection of the best set of individual target response spectrum out of 5,000 Monte Carlo generated sets of 7 of response spectra:

$$Error_i = \Xi_i + \Theta_i \tag{1}$$

where Ξ_i and Θ_i are formulated as follows:

$$\Xi_i = \sum_{j=1}^{Np} \left(\log\left(SA_j^T\right) - \log\left(SA_{i,j}^S\right)\right)^2 \quad (2)$$

$$\Theta_i = \sum_{j=1}^{Np} \left(\log\left(\sigma_j^T\right) - \log\left(\sigma_{i,j}^S\right)\right)^2 \quad (3)$$

where *Np* is the number of the spectral periods, SA_j^T is the value of the target (UHRS) at the spectral period of (T_j), $SA_{i,j}^S$ is the average of the j^{th} simulated individual target set at the spectral period of (T_j), σ_j^T is the value of the target standard deviation at the spectral period of *(T_j)*, and $\sigma_{i,j}^S$ is the standard deviation of the i^{th} simulated individual targets at the spectral period of *(T_j)*. The set of 7 that yields the minimum total error is selected as the target response spectra and will be used to select and scale appropriate GMs. Figure 3-5 shows the selected set of individual target response spectra that have the lowest error among 5,000 simulated sets.

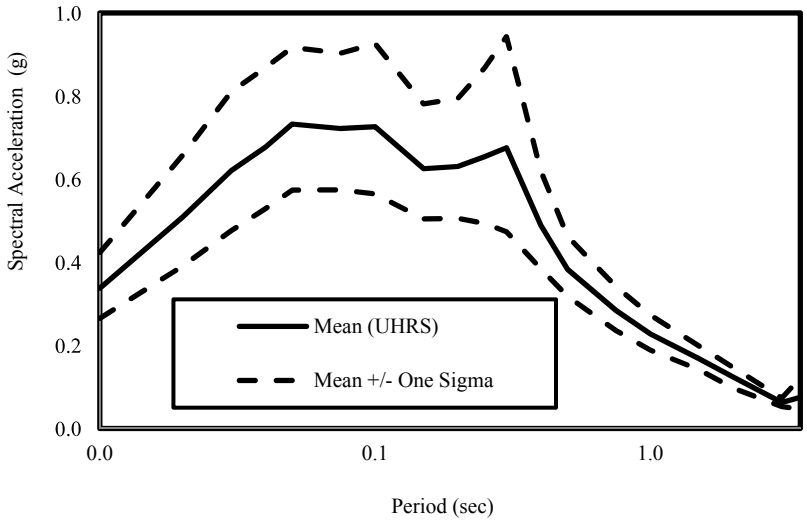

Figure 3-4. The UHRS for 2% probability of exceedance and the limits associated with $\pm\sigma$ of the mean.

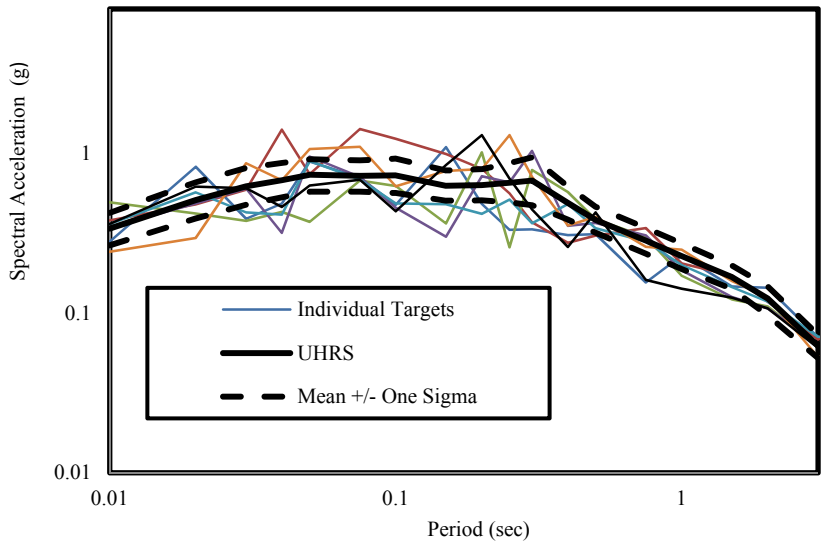

Figure 3-5. Individual set of target response spectra.

3.4 Seismological Parameters

In the literature, there are different constraints on the candidate earthquakes. The most important parameters that researchers address in their studies and that I also address in this study are the earthquake magnitude, source to site distance, and scaling limits. In this section I first review available research studies in this area and then set suitable values for parameters that are appropriate for the study site.

3.4.1 Scaling

Scaling of the GM is an effective way to make available GM time-histories match the 7 individual targets. Two main methods of scaling have been developed (Evangelos et al. 2010): time-domain and frequency-domain scaling. In this study, I scale the amplitude of GM response spectrum, which is a special case of the time-domain scaling method. Although it is widely accepted that the closer the scale factor to unity the better, there are different guidelines available on scaling limits of GMs. Lamprey and Abrahamson

(2006) studied the selection of GMs and they concluded that the limitation on scaling factors is appropriate when magnitude, distance, and site conditions are the only considered parameters.

I review two main amplitude scaling methods in my study. The first one is the single scale factor (*S.F.*) method where the whole GM's response spectrum is scaled by a scalar so that it exactly matches the target response spectrum at just one period, usually at the fundamental period of the structure (Baker 2010):

$$S.F. = \frac{SA_i^T}{SA_i^{GM}} \tag{4}$$

where SA_i^{GM} is the spectral acceleration of the GMs in the database at the spectral period T_i. The selection of T is another potential challenge for the selection of GM. The parameter T is usually taken as the fundamental period of structure, and if the response parameter of structure is sensitive to another period or a range of periods then there is a possible chance of underestimating the target with this method of scaling acceleration time-history (Baker 2010).

The second method is to scale GM's response spectrum over a range of periods instead of just one period. This method shifts the GM's response spectrum so that it has an overall fit of target over a period range. This range is usually defined by the seismic codes. The formulation for the scaling factor is as follows:

$$S.F. = \frac{\sum_{i=n_1}^{n_2} SA_i^T}{\sum_{i=n_1}^{n_2} SA_i^{GM}} \tag{5}$$

where n_1 and n_2 are the numbers associated to the minimum and the maximum of the period range. For the study site, the second method resulted in lower values of the root mean square (rms) error. For this example, GMs in the database will be scaled to have an overall fit of the individual target from spectral periods range of 0.15 seconds through 2.00 seconds (n_1=8 and n_2=17). This type of scaling does not change the original characteristics of the GM and there is no change in the phase.

3.4.2 Dominant Hazard Scenario

The selection of earthquakes from a database is usually based on the similarity of the seismological parameters between the study site and the selected earthquakes. Researchers address the two most important parameters in the selection of GMs for dynamic analysis of structures in their studies: the earthquake's magnitude and the source to site rupture distance. Other parameters such as fault mechanism, focal depth, tectonic environment, and site classification can also be defined to play a role in the GM selection procedure but these were not considered in this study.

Earthquake magnitude is an influential parameter in the GM selection, and most properties of a GM such as duration, the spectral shape, amplitude, and the frequency content is related to this parameter; but there are different recommendations about the level of flexibility on the limits that magnitudes of candidate GMs can have. Stewart et al. (2001) concluded that the magnitude of an earthquake is an important parameter in selection of GMs, and suggested a range of plus and minus 0.25 around the target magnitude (which comes from the deagreggation analysis and will be defined later) for the selection purposes. On the other hand, Shome et al. (1998) showed that a wider magnitude range is acceptable in the selection process without having any side effects.

Determining a tight or wide magnitude range will affect the size of the database but it does not affect the selection procedure of the proposed method. Deagreggation data is another product of a PSHA, which reflect the contribution of various possible scenarios (magnitude and source to site distance) to the seismic hazard at a site. Using deagreggation data, one can determine which magnitude and distance range have the dominant contribution to the hazard at a specific site, and use those values as the target values of magnitude and source to site distance at different spectral periods. I used the USGS online tool (https://geohazards.usgs.gov/deaggint/2008/) to conduct deagreggation analysis for the study site. Table 3-1 presents the deagreggation data obtained for the study site and for spectral accelerations of engineering interest (*i.e.,* 0.2, 0.5, 1.0, and 2.5 sec).

Table 3-1. Deagreggation data for the study site

	Deagreggation Results			
	P=0.2 sec	P=0.5 sec	P=1.0 sec	P=2.5 sec
Magnitude	7.3	7.5	7.6	7.6
Distance (*km*)	54.4	59.0	61.1	63.1

The deagreggation data summarized in Table 3-1 suggest that the dominant earthquake scenario for the study site is not sensitive to the spectral period. Therefore, to be consistent with the deagreggation analysis, I considered 7.0 to 7.8 for the magnitude range and 45 to 65 *km* for the distance range for the study site. GMs with magnitude and distance outside this range are excluded from candidate earthquakes.

3.5 Selection of GMs

3.5.1 Real Earthquake Database

I used the Pacific Earthquake Engineering Research Center (PEER) Next Generation of Attenuation (NGA) project strong-motion database for the selection of real earthquakes. A total of 3550 GMs and their seismological parameters are available in the database. Out of GMs available in this database, I only used earthquakes that not only fall inside determined magnitude-distance bin for the study site, but also have a scale factor more than 0.5 and less than 4. Limits on the scaling factor are varying from project to project and the size of database and is not the focus of my study. As the data from NGA-East becomes available, one should use it instead of NGA for sites located within the central and Eastern United States.

Each GM in the database is scaled and the error between the GM and the individual response spectrum is calculated. There are different measurements of dissimilarities between the GM and the target (*e.g.,* Evangelos et al. 2010; Bommer and Acevedo 2004). I used equation (6) to find the error between each individual target response spectrum and all the GMs in the database and chose the one with the least error. The same procedure is done for all the individual target response spectra to find the appropriate set of earthquakes for the time-history analysis.

All the GMs in the database are first scaled using equation (5) and then the error for each GM is defined as the square of the difference between the log of the individual target response and the log of GM response at all the spectral periods:

$$E = \sum_{i=1}^{Np} \left(\log\left(SA_i^{GM} \right) - \log\left(SA_i^{I.T.} \right) \right)^2 \qquad (6)$$

where SA_i^{GM} and $SA_i^{I.T.}$ are the values of the response of GM and the response of the individual target at the spectral period of T_i, respectively. Equation (6) is evaluated for all GMs in the database for each of the seven individual targets, and the result is 7 GMs that fit closely with one of the individual targets. Therefore, the selected set of 7 GMs has a mean close to UHRS and a variance close to the target at desired spectral periods. Figure 3-6 shows response spectra of the GMs selected from the database of real GMs. Figure 3-7 illustrates the response acceleration of the target, the mean of the 7 individual targets, and the mean of the 7 selected GMs from the NGA database. Figure 3-7 suggests a reasonable match between all three curves. Figure 3-8 shows time-histories of the selected GMs from the real earthquake database.

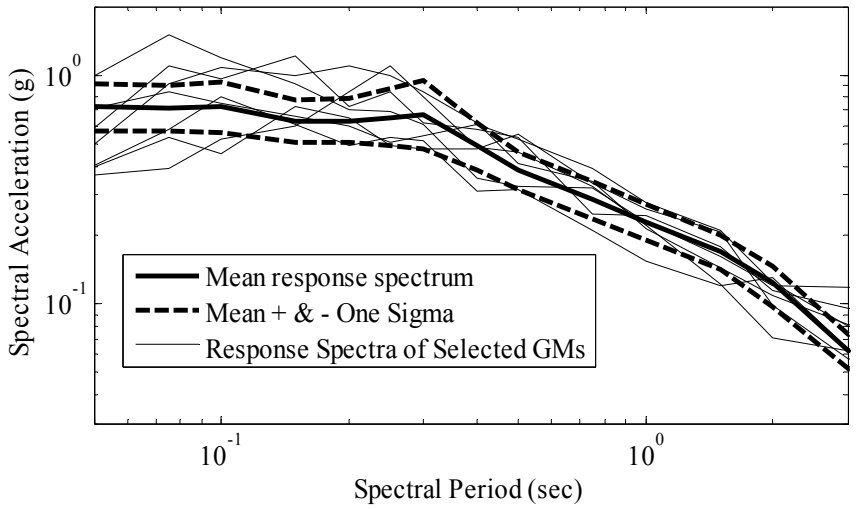

Figure 3-6. Selected GMs' response spectra of the real GMs from the NGA database.

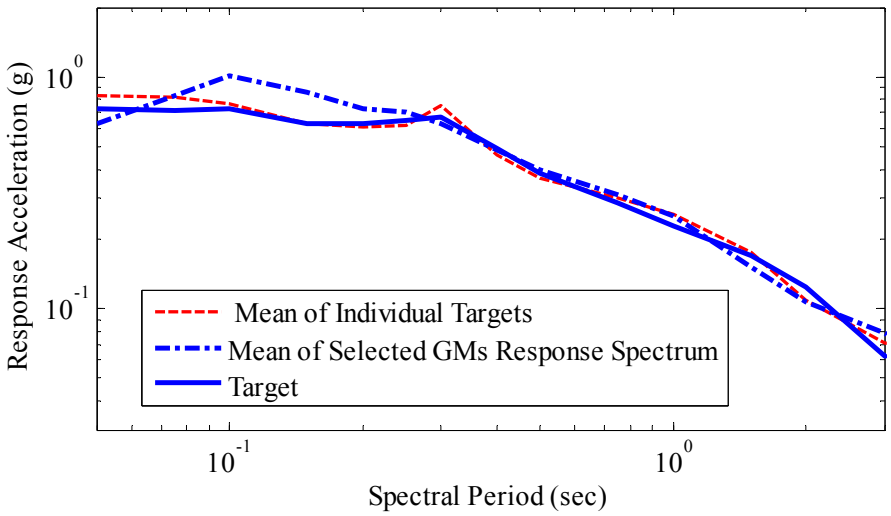

Figure 3-7. Target, mean of the individual selected targets, and the mean of the selected GMs from the NGA database.

3.5.2 SMSIM Database

An alternative category of candidate database GMs are those generated using the stochastic point-source procedure. The stochastic point-source procedure has been shown to yield acceptable results for the central and northern United States (*e.g.,* Hanks and McGuire 1981; Silva et al. 1997). The computer program SMSIM, available online at http://www.daveboore.com/, is used to generate earthquake acceleration time series. The computer program SMSIM generates GMs based on the seismological parameters of a region including: source, path, and site effects. To generate candidate earthquakes, engineers should have a good knowledge of the seismological parameters of the study region. Some experts argue that knowledge of the input parameters are beyond the knowledge of practicing engineers. However, since the time-history analysis is for important structures, the input seismological parameters are available and determined by seismological studies that are necessary for such infrastructures.

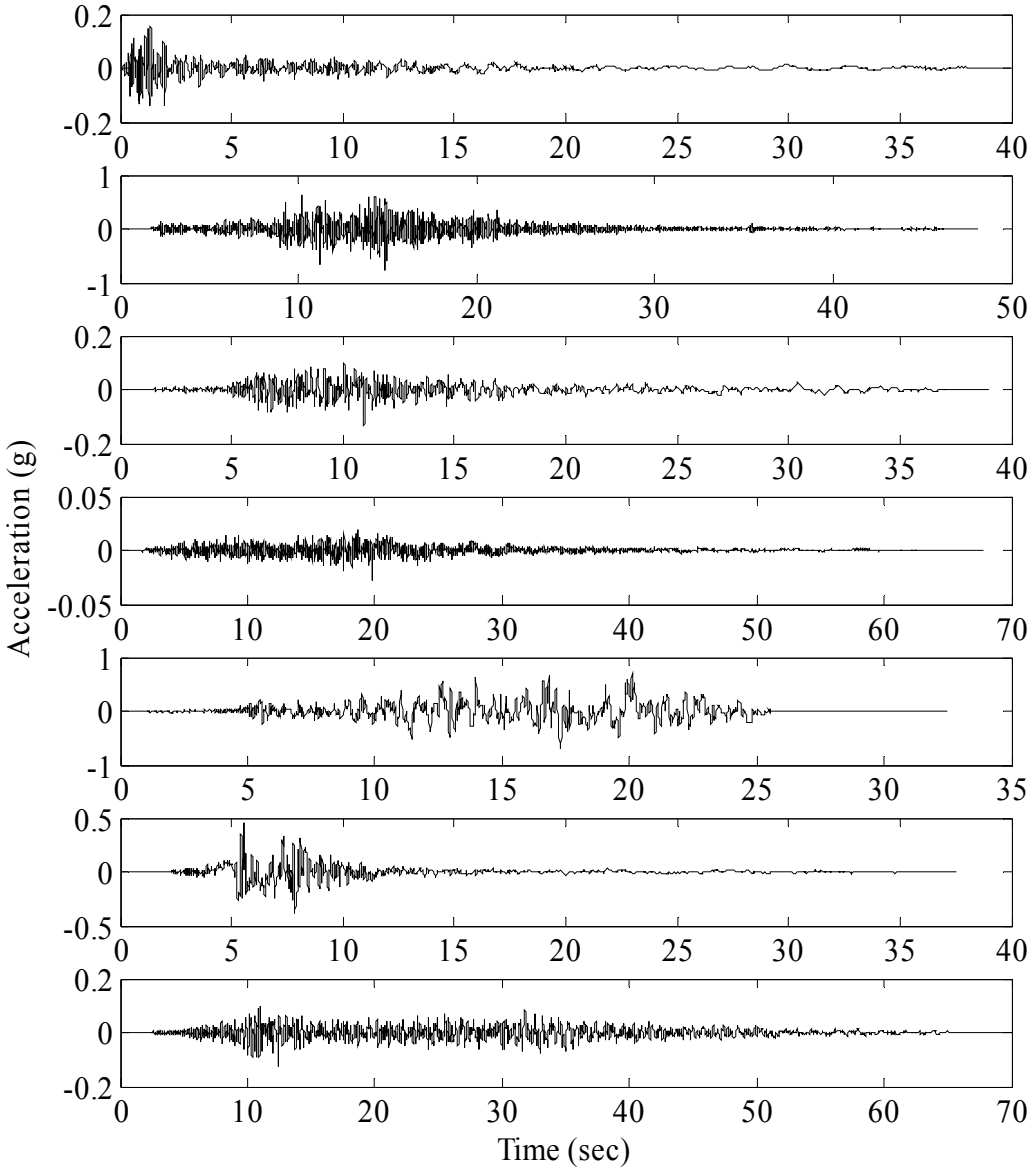

Figure 3-8. Time-histories of the selected GMs using the NGA database.

Table 3-2 presents parameters used as input to the computer program SMSIM. The magnitude and source to site distance were chosen in the way to be consistent with the dominant earthquake scenario obtained from the deagreggation of the study site. Other values of the table are adopted from Atkinson and Boore (2006).

Table 3-2. Source, site, and path parameters used by Atkinson and Boore (2006) to develop ground motion model for ENA. I used the same values for generation of candidate earthquake from SMSIM and EXSIM codes.†

Parameter	Value
Magnitude	7.0-7.8
Distance	45-65 *km*
Shear-wave velocity, β	3.7 *km/sec*
Density (at 13 *km* depth)	2.8 g/cm^3
Rupture propagation speed	0.8β
Stress parameter	140 bars
Pulsing percent *	50%
Kappa	0.005
Geometric spreading	-1.3(0-70 *km*)
	0.2(70-140 *km*)
	-0.5(>140 *km*)
Distance dependence of duration	0.0(0-10 *km*)
	0.16(10-70 *km*)
	0.03(70-130 *km*)
	0.04(>140 *km*)
Slip distribution / hypocenter location	Random
Fault dip *	50°
Fault length and width *	30×9
Fault subdivision into subsources *	15×4
Quality factor	$Q=max(1000,893f^{0.32})$

†The parameters marked with * correspond specifically to the stochastic finite-fault modeling in EXSIM, while other parameters are used both in EXSIM and SMSIM. Fault length and width and fault subdivision values have been slightly changed.

I modified the computer program SMSIM so that it can be run repeatedly without asking for input and generates the requested number of GMs. Using the parameters listed in Table 3-2, 450 earthquakes were generated for the database of candidate earthquakes. I treat the earthquakes from the point-source stochastic model in the same manner as real earthquakes. First, each record is scaled and then the GM with the best match to the individual target is selected. The selected and scaled GMs from the stochastic point-source database are plotted in Figure 3-9. Figure 3-10 illustrates the response

acceleration of the target, the mean of the 7 individual targets, and the mean of the 7 selected GMs from the SMSIM database.

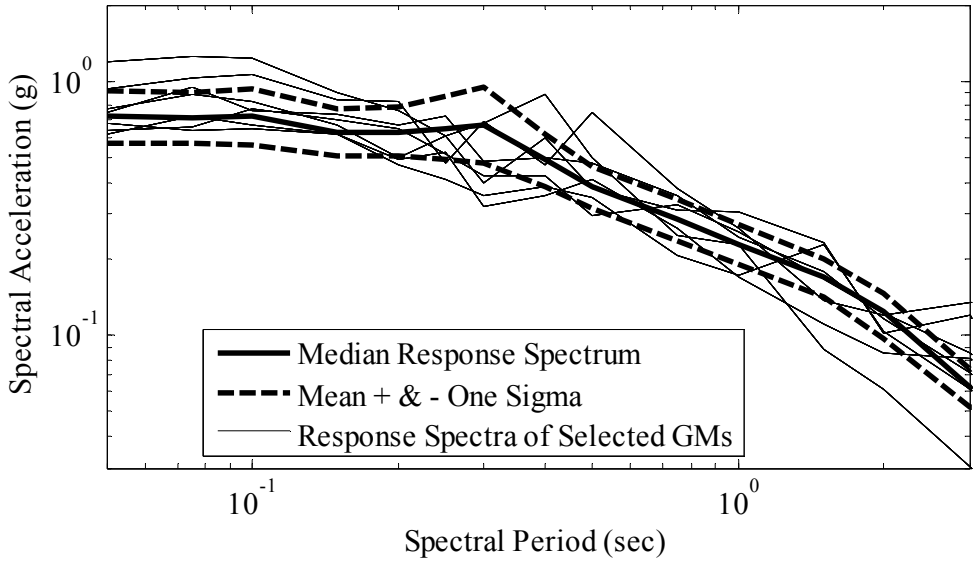

Figure 3-9. Selected GMs' response spectra from the SMSIM generated database.

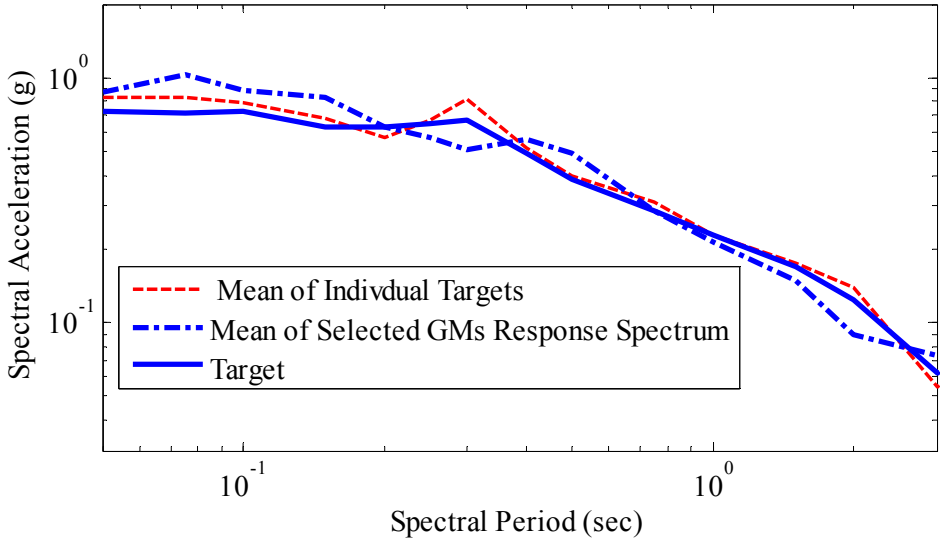

Figure 3-10. Target, mean of the individual selected targets, and the mean of the selected GMs from the SMSIM database.

3.5.3 EXSIM Database

Another synthetic method that is used in this research to generate candidate GMs is the stochastic finite-fault model. This model was developed initially by Beresnev and Atkinson (1998a) and later updated by Motazedian and Atkinson (2005) to correct the dependency of the original method to subfault dimensions. The finite-fault model is developed to take into account the near source effects on the earthquake's acceleration time-history. The basic concept of finite-fault modeling is that it divides the fault area into a number of subfaults and treats each sub fault as a point-source, and applies the point-source model to generate an acceleration time series for each subfault and adds up the acceleration time-history from each subfault with an appropriate time shift. Boore (2009) compared the stochastic point-source and finite-source GM simulations and modified the EXSIM computer code to result in better estimates of GM time-history and spectral acceleration. The computer program used to generate synthetic GMs is available at http://www.daveboore.com/. In this case, the deagreggation data presented in Table 3-1 implies that since the study site and the dominant source scenario is not far away, the finite-fault model is applicable to this example. Table 3-2 also lists the input parameters used in this study. A total of 250 earthquakes are produced to serve as candidate earthquakes. The response spectra of the selected and scaled ground motions from the database of EXSIM are shown in Figure 3-11. The spectral acceleration of the mean of the selected GMs, target response spectral, and mean of the individual targets are compared in Figure 3-12.

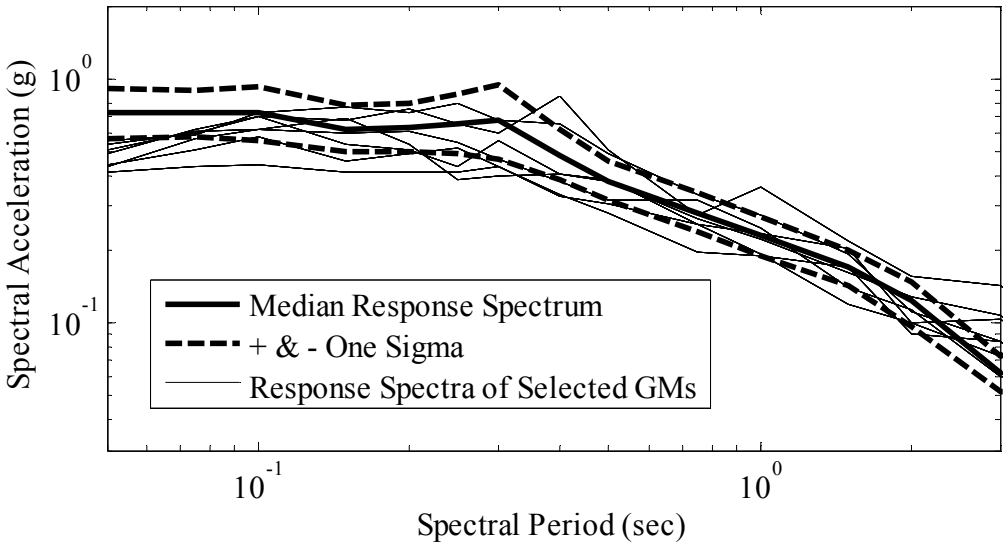

Figure 3-11. Selected GMs' response spectra from the EXSIM generated database.

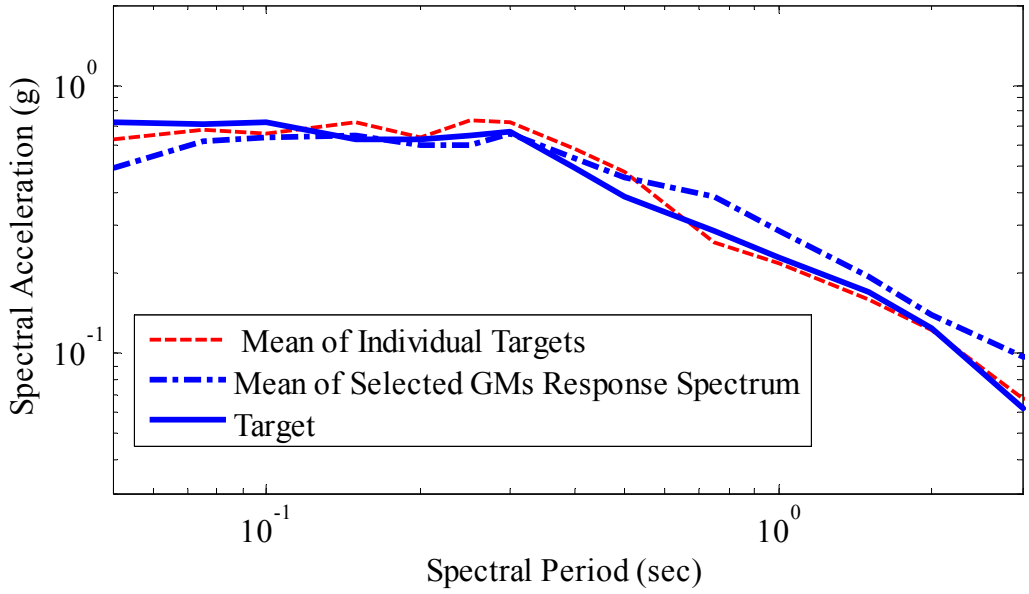

Figure 3-12. Target, mean of the individual selected targets, and the mean of the selected GMs from the EXSIM database.

3.6 Summary and Conclusions

A step-by-step method for the selection of GMs for the time-history analysis is presented in this study. The procedure considers the variability of the target response based on different possible hazard scenarios and includes the measured variability in the GM selection procedure. The method includes the variability of the target in the GM selection procedure with the help of the individual target response spectra. The details of the proposed procedure are discussed through an example. I first defined the target for the study site using the PSHA analysis. I capture the variability of the target (UHRS) through a logic tree defined for the study site. Separate PSHA analyses are conducted for each branch of the logic tree, and hazard curves associated with the mean and mean $\pm 1\sigma$ are used as the target, the upper and the lower limits of the target. A Monte Carlo simulation is used to generate 7 individual targets response spectra with the mean and standard deviation of the target. The mean and the standard deviation of the generated suite is improved by simulating a large number of the individual target sets and selecting the set with closest mean and standard deviation with the target's mean and standard deviation. These 7 individual response spectra will be treated as target spectra. In other words, I will have 7 individual target spectra rather than one. Recorded GMs with similar seismological characteristics of the study site as well as GMs generated using stochastic point-source model and stochastic finite-fault model are used as the candidate GMs for the time-history analysis. The candidate synthetic GMs (*i.e.* SMSIM and EXSIM generated GMs) are simulated using the dominant magnitude and source to site distance obtained from the deagreggation analysis. Since synthetic methods consider the seismological parameters of the study area in simulation of GMs, those characteristics is

considered in the structural response by using GMs from synthetic methods in time-history analysis.

3.7 References

AASHTO (2004). LRFD Bridge Design Specifications and Interim Specifications. 3rd Edition, LRFDUS-3-I2. American Association of State Highway and Transportation Officials, Washington, DC.

Atkinson, G. M., and Boore, D. M. (2006). "Earthquake ground-motion prediction equations for eastern North America." *Bulletin of the Seismological Society of America*, 96, 2181-2205.

Baker, J. W. (2010). "The conditional mean spectrum: a tool for ground motion selection." *ASCE Journal of Structural Engineering (in press).*

Baker, J. W., and Cornell, C. A. (2006). "Spectral shape, epsilon and record selection." *Earthquake Structure Dynamics,* 35, 1077-1095.

Boore, D. M. (2003). "Simulation of ground motion using the stochastic method." *Pure and Applied Geophysics,* 160, 635-676.

Boore, D. M. (2009). "Comparing stochastic point-source and finite-source ground-motion simulations: SMSIM and EXSIM." *Bulletin of the Seismological Society of America,* 99, 3202-3216.

Beresnev, I., and Atkinson, G. (1998a). "FINSIM: a FORTRAN program for simulating stochastic acceleration time histories from finite faults." *Seismic Research Letters,* 69, 27-32.

Bommer, J. J., and Acevedo A. B. (2004). "The use of real earthquake accelerograms as input to dynamic analysis." Journal of Earthquake Engineering, 8(4), 1-50.

Campbell, K. W. (2003). "Prediction of strong ground motion using the hybrid empirical method and its use in the development of ground-motion (attenuation) relations in eastern North America." *Bulletin of the Seismological Society of America,* 93, 1012-1033.

Federal Emergency Management Agency (FEMA). NEHRP Recommended Provisions for Seismic Regulations for New Buildings and Other Structures. FEMA 450, Part 1: Provisions, Part 2: Commentary. Building Seismic Safety Council, Washington, D.C. 2003 edition.

Hanks, T. C., and McGuire, R. K. (1981). "The character of high-frequency strong ground motion." *Bulletin of the Seismological Society of America,* 71, 2071–2095.

Iervolino, I., and Cornell, C. A. (2005). "Record Selection for Nonlinear Seismic Analysis of Structures." *Earthquake Spectra,* 21, 685-713.

Jayaram, N., Lin, T., and Baker, J., (2011). "A Computationally Efficient Ground-Motion Selection Algorithm for Matching a Target Response Spectrum Mean and Variance." *Earthquake Spectra,* 27(3), 797-815.

Katsanos E. I., Sextos, A. G., and Manolis, G. D. (2010). "Selection of earthquake ground motion records: A state-of-the-art review from a structural engineering perspective." *Soil Dynamics and Earthquake Engineering,* 30, 157-169.

Lamprey, J. W, and Abrahamson, N. (2006). "Selection of ground motion time series and limits on scaling." *Soil Dynamics and Earthquake Engineering,* 26, 477-482.

Motazedian, D., and Atkinson, G. M. (2005). "Stochastic finite-fault modeling based on a dynamic corner frequency." *Bulletin of the Seismological Society of America,* 95, 995-1010.

Naeim, F., Alimoradi, A., and Pezeshk, S. (2004). "Selection and Scaling of Ground Motion Time Histories for Structural Design Using Genetic Algorithms." *Earthquake Spectra,* 20, 2, 413-426.

Pagliaroli, A., and Lanzo, G. (2008). "Selection of real accelerograms for the seismic response analysis of the historical town of Nicastro (Southern Italy) during the March 1638 Calabria earthquake." *Engineering Structures,* 30, 2211-2222.

Petersen, M. D., Frankel, A. D., Harmsen, S. C., Mueller, C. S., Haller, K. M., Wheeler, R. L., Wesson, R. L., Zeng, Y., Boyd, O. S., Perkins, D. M., Luco, N., Field, E. H., Wills, C. J., and Rukstales, K. S. (2008). "Documentation for the 2008 Update of the United States National Seismic Hazard Maps." Open-File Report 2008-1128.

Sabetta, F., Lucantoni, A., Bungum, H., and Bommer, J. J. (2005). "Sensitivity of PSHA results to ground motion prediction relations and logic-tree weights." *Soil Dynamic and Earthquake Engineering,* 25, 317-329.

Shome, N., Cornell, C. A., Bazzurro, P., and Carballo, J. E. (1998). "Earthquake, records and nonlinear responses." *Earthquake Spectra,* 14(3), 469-500.

Silva, W. J., Abrahamson, N., Toro, G., and Costantino, C. (1997). Description and validation of the stochastic ground motion model, Report submitted to Brookhaven National Laboratory, Associated Universities, Inc. Upton, New York 11971, Contract No. 770573.

Stewart, J. P., Chiou, S. J., Bray, J. D., Graves, R. W., Somerville, P. G., and Abrahamson, N. A. (2001). "Ground motion evaluation procedures for performance-base design." PEER report 2001/09, Pacific Earthquake Engineering Research Center, University of California, Berkeley.

Tavakoli, B., and Pezeshk, S. (2005). "Empirical-stochastic ground-motion prediction for eastern North America." *Bulletin of the Seismological Society of America,* 95, 2283-2296.

4 Vertical to Horizontal Ratio Model for the Mississippi Embayment

4.1 Introduction

Seismic codes require the effects of the vertical component of ground motions to be considered in the analysis and design of critical structures. The effects of vertical component of ground motions on structures are addressed in different studies such as Kunnath et al. (2008) and Bozorgnia and Campbell (2004a). In the same way as the horizontal design, the vertical design and analysis of structures needs a vertical design spectrum which reflects the main seismological characteristic of the region. There are two main approaches in developing a vertical design spectrum for a study site (Gülerce and Abrahamson 2011; Bommer et al. 2011). The first approach is to follow the same procedure as is used for the horizontal Probabilistic Seismic Hazard Analysis (PSHA) but use the vertical Ground Motion Prediction Equations (GMPEs) to estimate the vertical hazard at different periods. The main disadvantage of this first approach is the absence of up-to-date vertical GMPEs in most regions. For instance, there is no vertical GMPE developed for regions such as the Central and Eastern United States. Another problem with this approach is a possible mismatch between the horizontal and vertical dominant hazard scenarios (magnitude and distance) which can be confusing in ground motion selection for time-history analysis. The second method is to use the V/H ratio of the ground motion to scale an available horizontal design spectrum to a vertical spectrum.

The V/H ratio technique was applied by Nakamura (1989) in estimating the dynamic properties of soil layers. He used the ratio of the horizontal to vertical of the micrometers to estimate the soil's transfer function. The validity of this assumption was proved using micrometer observation results. Nakamura calculated the seismic

characteristics of the soil along about a 1500 *km* section of the Japan railway lines using the horizontal to vertical ratio method. Lermo and Chavez-Garcia (1993) used the horizontal to vertical ratio technique to estimate the empirical transfer function without the reference station. They also concluded that if site effects are caused by geology, an estimate of the dominant period of the site and the local amplification can be obtained using the records of only one station.

Niazi and Bozorgnia (1992) studied a large number of V/H response spectra of the earthquakes available at the Taiwan strong motion array. They investigated the effects of the magnitude and source to site distance on the V/H ratio. They concluded that the spectral period has a large effect on the V/H ratio. They suggested the peak of the V/H ratio exceeds a value of 2/3 in the near source regions. They also studied V/H ratio from the Loma Prieta and the Northridge earthquake for both soil and rock sites and suggested that the general pattern of the V/H ratio, such as having a distinct peak at low spectral periods and the value of the peak which they suggest to be 2/3, is universal. At longer periods the V/H ratio increases slowly. Bozorgnia and Niazi (1995) made the following observations: that V/H ratio is a function of spectral period, distance to the fault, and earthquake magnitude, and that the V/H ratio is largest at short periods in near-field regions. In the near-field region, the peak of the V/H ratio is larger than the ratio of the peak ground accelerations. In the short period range, the 2/3 value underestimates the V/H ratio, especially in near-field regions, and at long periods the V/H ratio falls below 2/3.

Atkinson (1993) used small magnitude earthquakes recorded at distances beyond 20 *km* on rock site conditions to develop an empirical model of the V/H ratio for the

Central and Eastern United States. Atkinson (1993) studied the V/H ratio of the Fourier amplitude for the rock site conditions. For the Saguenay earthquakes the V/H ratio is between 0.7 and 1.0, suggesting a higher ratio in the Central and Eastern United States in comparison with the Western United States at large distances. According to Atkinson (1993), the general pattern of the V/H ratio in the 1.0 to 10.0 Hz frequency range has an opposite trend compared to the Western United States. Atkinson (1993) also concluded that the magnitude dependency of the V/H ratio model for the Central and Eastern United States is smaller compared to the Western United States.

Seismic codes suggested a variety of V/H models to obtain the vertical design spectrum. Regulatory Guide 1.6 (1973) is among the first codes that consider obtaining the vertical design spectrum from the horizontal spectrum using the V/H ratio model. Regulatory Guide 1.6 assumes different values of V/H for short periods and long periods. McGuire et al. (2001) studied the V/H ratio for both the Western United States and the Central and Eastern United States to update the Regulatory Guide 1.6 values for the V/H ratio. They studied recordings of the Saguenay event and the only three available recordings of the Nahanni and Gazli earthquakes for the Central and Eastern United States. To develop recommended values for applications for the Central and Eastern United States, the simple point-source model was extended to consider P-SV waves and the model was used to estimate the vertical component of the spectra. They validated their model with observations at rock sites from the 1989 magnitude 6.9 Loma Prieta earthquake. The general trend of the model is very close to the Western United States model which is derived empirically. They developed recommended V/H models for the Western and Central and Eastern United States which is dependent on the expected Peak

Ground Acceleration (*PGA*) of the earthquakes. They suggested that magnitude dependencies of the V/H ratio in the Central and Eastern United States are smaller in comparison with Western United States; and they relate the difference to the fact that in the Western United States, the V/H model did not include the magnitude saturation apart from the stress drop that decreases with the increasing magnitude.

Gülerce and Abrahamson (2011) developed a GMPE to predict the V/H ratio. They reviewed methods for constructing the site-specific vertical design spectra from a Uniform Hazard Spectrum (UHS) and Conditional Mean Spectrum (CMS) to be consistent with the PSHA. The functional form of the GMPE for the V/H ratio is consistent with the horizontal GMPE developed by Abrahamson and Silva (2008). They used the NGA database which consists of 2684 sets of recordings from 127 earthquakes. Their functional form to predict the V/H ratio is dependent on the earthquake magnitude, source to site distance, and type of faulting. They also included the functional form developed by Walling et al. (2008) to predict the effects of the nonlinear soil behavior in the V/H ratio model.

Bommer et al. (2011) reviewed current models for the V/H ratio by different seismic codes and regulations such as the Regulatory Guide 1.6, McGuire et al. (2003), the EC8 (Eurocode 2008), and the National Earthquake Hazards Reduction Program (NEHRP 2009). They also developed a model for the V/H ratio for Europe and the Middle East. They found a simple functional form, expressing the V/H ratios as a function of magnitude, the style of faulting (reverse, normal, and strike-slip), the source to site distance, and the site class to appropriately describe the V/H model. Their proposed model is based on 1296 accelerograms from 392 events occurring in Europe,

the Middle East, and surrounding regions, and predicts V/H ratios for *PGA* and spectral accelerations from 0.02 to 3.0 seconds. Although their model predicts lower values for V/H ratio, it has general agreement with the model developed by Gülerce and Abrahamson (2011), which is based on the data from Western North America. Their model can be used for a magnitude range of 4.5 to 7.6 and distances up to 100 *km*.#

In the present study, I developed a model to estimate the V/H ratios for the Mississippi embayment. The resulting GMPE can be used in developing a site-specific vertical design spectrum for the study area from a horizontal design spectrum. The proposed model is based on a database of ground motions with magnitude ranging from 3.5 to 5.6 and source to site distances up to 900 *km*, and covers 23 spectral periods from 0.0 (*PGA*) to 10.0 seconds. The functional form used to predict V/H values is consistent with the horizontal GMPE developed by Pezeshk et al. (2011).

4.2 Database

To perform V/H ratio analysis, earthquakes are selected from two different complementary databases. The first group is earthquakes located within the Mississippi embayment boundary, and the second group is earthquakes suggested by the NGA-East database working group.

4.2.1 Earthquakes Located in the Mississippi Embayment

The New Madrid seismic zone is the main seismic zone in the Central United States. This seismic zone has generated three large events in 1811-1812 with estimated moment magnitudes of 7.5 to 7.8 (Bakun and Hopper 2004; Cramer and Boyd 2012) and has generated small to moderate earthquake ground motions in the past few years. Eleven earthquakes, with moment magnitudes of 3.5 and larger that occurred after 2000,

were selected from the Center for Earthquake Research and Information (CERI) database (available at: http://www.ceri.memphis.edu/). The list of earthquakes and their magnitudes along with their locations are summarized in Table 4-1. Ground motions for V/H analyses are obtained from stations that are located within the Mississippi embayment and surrounding areas. This decision was made so that the resulting V/H model captures the deep soil response of the study area. Figure 4-1 shows the map of the Central United States with the location of the stations as well as the Mississippi embayment boundary.

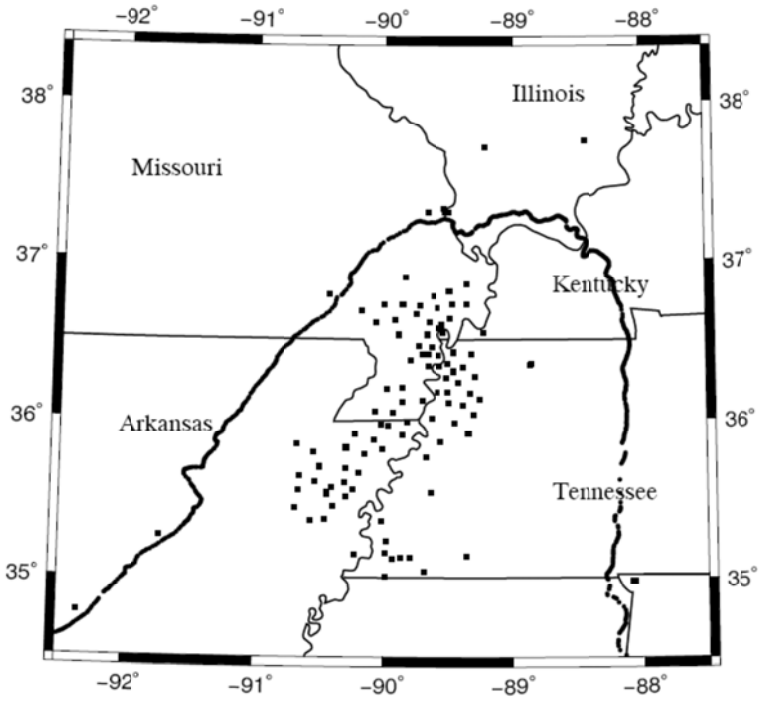

Figure 4-1. Location of stations used in this study

Table 4-1. List and details of earthquakes with magnitude greater than 3.5 from the CERI database.

Date	Magnitude	Lon	Lat	Location
30/4/2003	4	35.94	-89.92	1.42 *km* north of Blytheville, AR
6/6/2003	4	36.88	-88.99	2.65 *km* east of Bardwell, KY
10/2/2005	4.1	35.76	-90.25	2.27 *km* south of Milligan Ridge, AR
1/5/2005	4.2	35.83	-90.15	2.57 *km* south of Big Lake, AR
2/6/2005	4	36.15	-89.47	2.45 *km* southwest of Miston, TN
20/6/2005	3.6	36.92	-89.00	4.15 *km* southwest of Blandville, KY
2/1/2006	3.6	37.84	-88.42	6.25 *km* northeast of Saline City, IL
2/3/2010	3.7	36.79	-89.36	1.58 *km* east of Whiting, MO
22/9/2011	3.6	36.82	-90.75	6.41 *km* northwest of Budapest, MO
21/2/2012	3.9	36.87	-89.42	4.81 *km* southeast of Bertrand, MO
29/10/2012	3.9	35.20	-90.63	2.47 *km* south of Flag Lake Crossing, AR

4.2.2 Earthquakes from the NGA-East Database

To have a better constrained V/H model, I decided to include ground motion time-histories from the NGA-East database. The NGA-East database consists of 85 events representing the source regions, magnitudes and world-wide analogs for the Central and Eastern United States. Earthquakes with longitudes within 34.5° and 38.5° and latitudes within -87.7° and -92.3° are selected from the NGA-East database so that the selected ground motions reflect the seismological parameters of the Central and Eastern United States and, more specifically, the Mississippi embayment. I also decided to include time-histories from the magnitude 5.6 Oklahoma event and its aftershock since it was the only relatively large magnitude earthquake that happened close to the study area. Table 4-2 summarizes details of the selected events from the NGA-East database. Therefore, the database of ground motions for the regression analysis consists of 560 time-histories with magnitudes 3.5 to 5.6 and the hypocentral distances of 10 to 900 *km*. A map of the

selected events along with the boundaries of states is shown in Figure 4-2. Details about the data processing and steps to prepare ground motion recordings can be found in Cramer (2008).

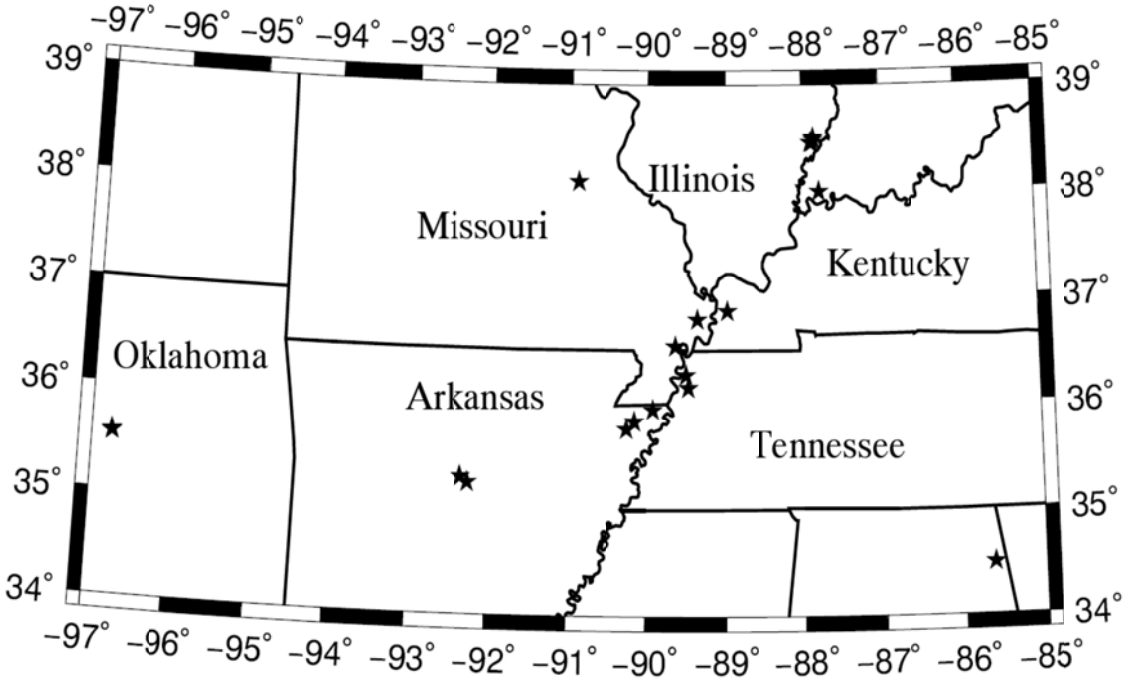

Figure 4-2. Location of earthquakes used from the NGA-East database.

Table 4-2. List and details of selected earthquakes from the NGA-East database.

Date	event	Mag	Lon	Lat
4/5/2001	Enola	4.34	35.24	-92.25
18/6/2002	Caborn	4.5	37.99	-87.78
29/4/2003	Ft Payne	4.59	34.49	-85.63
7/9/2006	Ridgely	3.41	36.27	-89.5
18/10/2006	Marston	3.47	36.54	-89.64
2/11/2006	Marvin	4	37.2	-81.92
18/4/2008	MtCarmelIL	5.32	38.45	-87.89
18/4/2008	MtCarmelAft	4.61	38.48	-87.85
21/04/2008	MtCarmelAft	4	38.5	-87.85
25/04/2008	MtCarmelAft	3.72	38.45	-87.87
15/10/2010	Guy	4.4	35.29	-92.34
20/11/2010	Guy	4.4	35.29	-92.34
6/11/2011	SparksOK	4.7	35.55	-96.75
5/11/2011	SparksOK	5.6	35.54	-96.75
7/6/2011	Sullivan	3.9	38.08	-90.9

I included all the available and applicable events in the regression analysis, but it should be noted that there are no events with magnitudes greater than 5.6 in the study. Since this result of the proposed model has not been verified with actual recordings of magnitudes greater than 5.6 for the study region, results from this study should be used with extra caution for such events.

4.3 Methodology

In this study, a model for the V/H ratio is developed for spectral periods of 0.0 (*PGA*) to 10.0 seconds. I estimated V/H values using the same periods used by Pezeshk et al. (2011). I calculated 5% damped response spectrum of vertical and horizontal components of motions in the database and used to develop a GMPE for V/H ratios. Study of the V/H ratio using the Fourier amplitude instead of response spectrum is also applied in different studies (Zandieh and Pezeshk 2011; Lermo and Chavez-Garcia 1993),

but developing the V/H ratio using the ratio of Fourier amplitude is used mostly for estimating the first dominant period of a site and the local amplification of ground motions.

The resultant V/H ratio model can be used to scale the available horizontal design spectrum to the site-specific vertical design spectrum as mentioned in Gülerce and Abrahamson (2011). Since both selected ground motions and recording stations are located within the Mississippi embayment, the resulting V/H ratio model includes both source characteristics and the site response of the region.

Zandieh and Pezeshk (2011) suggested that there are no discernible differences between using the north-south and the east-west components of ground motions in the study area, so in this study I performed V/H analyses using east-west components of ground motions.

The means of the observed V/H ratios are shown in Figures 4-3 and 4-4. In Figure 4-3, data is sorted based on the source to site distance, and data in Figure 4-4 is sorted to illustrate the effect of the magnitude in the V/H ratio values. I conducted regression analysis at each period independent of other periods using the maximum likelihood method (Joyner and Boore 1993). The sufficiency of the proposed V/H ratio model is verified through the analysis of residuals.

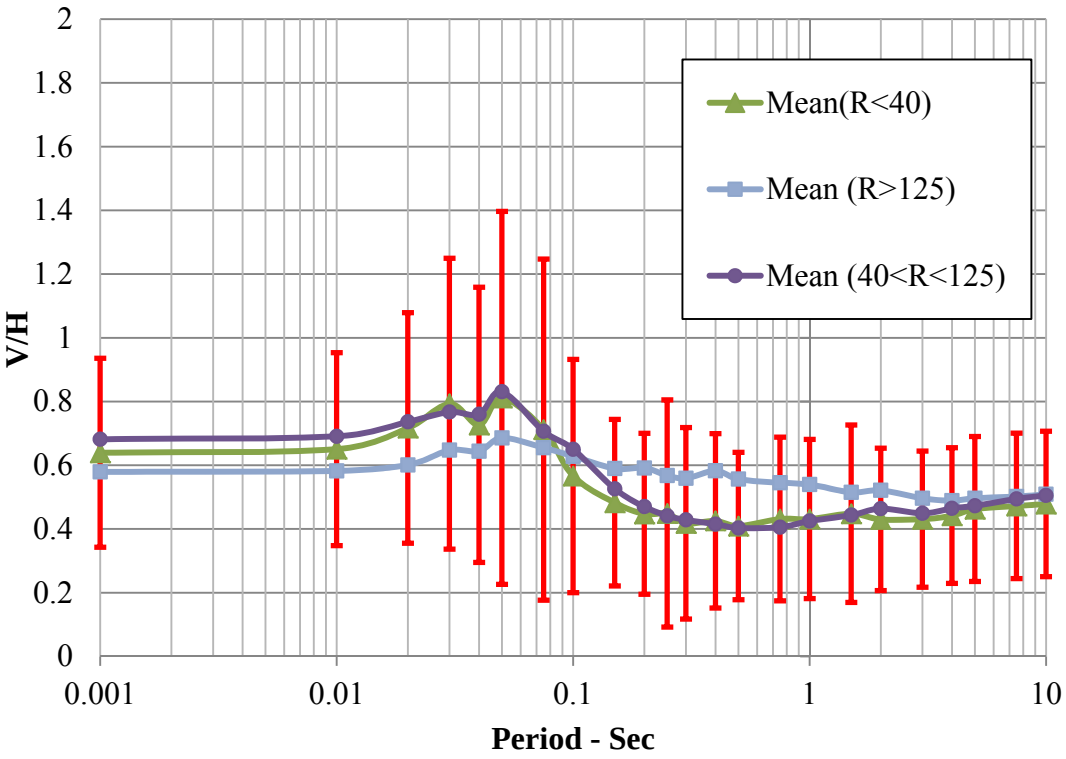

Figure 4-3. Effect of distance on the observed data. Limits of each bin is selected in such a way to have relatively the same number of data in each category. The error bars show standard deviations at each period and are only plotted for data with the source to site distances of less than 40 *km*

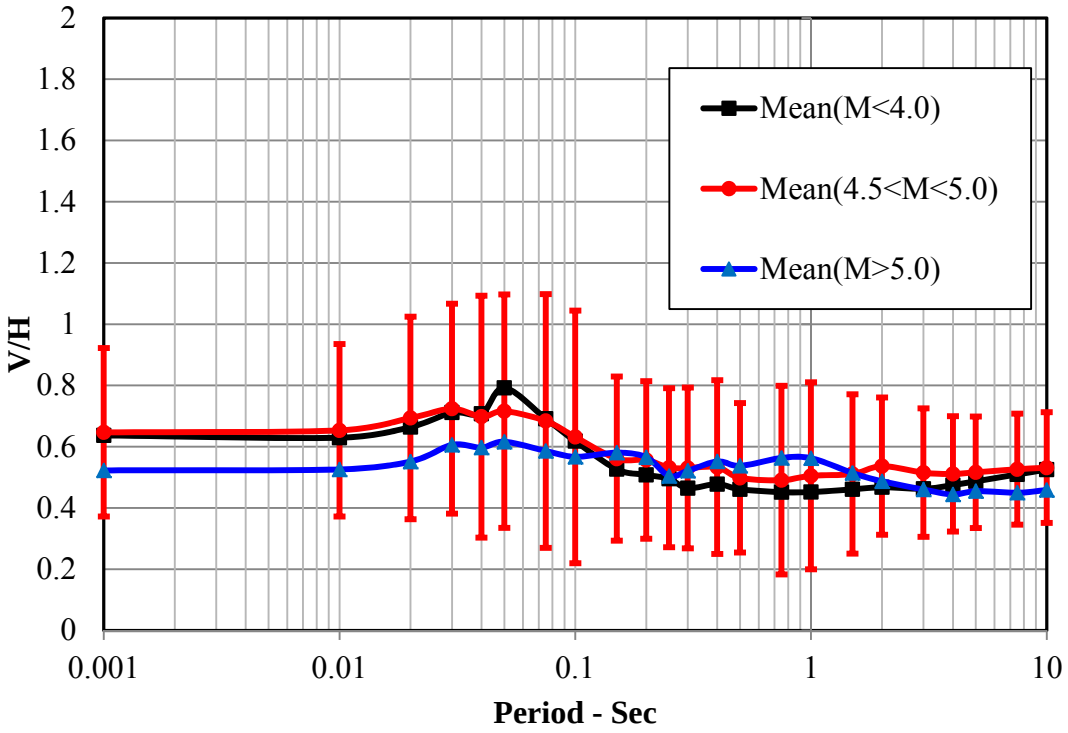

Figure 4-4. Effect of magnitude on the observed data. Limits of each bin is selected in such a way to have relatively the same number of data in each category. The error bars show standard deviations at each period and are only plotted for data with the magnitude between 4.5 and 5.0.

4.4 Parametric Model and Results

Using the results of V/H ratio analysis from actual earthquakes, a parametric model is proposed to estimate the V/H values within the study site. I used the magnitude, the distance, and the shear-wave velocity in the upper 30m as the input parameters for the proposed functional form. Generally, the functional form used to predict V/H ratios in a region are assumed in a way to be consistent with the functional form of the horizontal GMPEs developed for that area (Gülerce and Abrahamson 2011; Bommer et al. 2011). The functional form used in this study to predict the V/H ratio is consistent with the functional form used by Pezeshk et al. (2011), which is developed for the Central and

Eastern United States. To account for the nonlinear site effects (*i.e.,* effects of the V_{s30}) in the prediction of the V/H ratio, I decided to add the term developed by Boore et al. (1997) to the functional form developed by Pezeshk et al. (2011):

$$\begin{aligned}&\log(V/H) = a(1) + a(2)\times M_w + a(3)\times M_w^2 + \\ &\left(a(4) + a(5)\times M_w\right)\times \min\left(\log(R), \log(70)\right) + \\ &\left(a(6) + a(7)\times M_w\right)\times \max\left(\min\left(\log\left(\frac{R}{70}\right), \log\left(\frac{140}{70}\right)\right), 0\right) + \\ &\left(a(8) + a(9)\times M_w\right)\times \max\left(\log(\frac{R}{140}), 0\right) + a(10)\times R + a(11)\times \log(\frac{Vs30}{800}) + \varepsilon + \eta\end{aligned} \tag{1}$$

where

$$R = \sqrt{R_{rup}^2 + h^2} \tag{2}$$

In Equation (1), $a(1)$ through $a(12)$ are the regression coefficients, M_w is the moment magnitude, V_{s30} is the average shear-wave velocity in the upper 30*m* of soil profiles (*m/s*), h is the hypocentral distance (*km*), and ε and η represent the intra-event and inter-event variation, respectively. The ε and η are assumed to be normally distributed with variances $\sigma^2_{intra-event}$ and $\sigma^2_{inter-event}$. The total standard deviation is given by Equation (3):

$$\sigma_{\ln(V/H)} = \sqrt{\sigma^2_{\text{int}er-event} + \sigma^2_{\text{int}ra-event}} \tag{3}$$

Coefficients $a(1)$ through $a(12)$ are determined for each spectral period using the maximum likelihood method developed by Joyner and Boore (1993) which allows for correlation among subsets of the residuals. Joyner and Boore (1993) introduced a new computational method for one-stage and two-stage maximum likelihood analyses of strong motion data. They studied both one-stage and two-stage methods with the help of Monte Carlo analysis and concluded that both methods, if properly applied, are unbiased

and have comparable uncertainties. The general two-stage regression method is designed to include the concept of earthquake-to-earthquake component of variance by decoupling the magnitude dependency from the distance dependency. In the first stage, the distance dependency is determined along with the intra-event aleatory variability and a set of amplitude factors for each earthquake, and later in the second stage, the amplitudes factors are regressed against magnitude to determine the magnitude dependency as well as the inter-event variability. Joyner and Boore (1993) reexamined the two-stage method and derived the corrected weighting scheme for the second stage to give satisfactory results.

Bommer et al. (2011) and Gülerce and Abrahamson (2011) suggested a value of 5 and 10 for the hypothetical depth, respectively. I assumed a value of 6 for the *h* parameter to be consistent with the values of *h* derived in Pezeshk et al. (2011) which are estimated between 5.98 to 7.33 depending on the period. Since faults in the Central United States do not have the same characteristics as in the Western United States, I did not include type of faulting in the functional form.

The shear-wave velocity for the upper 30 meters is one of the input parameters of the functional form to predict the V/H response of the study area. The parameter V_{s30} for most of the stations used in this study area are known and used in the regression analysis. For the stations without a known V_{s30}, I assumed a value of 269 *m/s*, which is the average of the upper and the lower limits of the NEHRP site D category. This assumption has a general agreement with the shear-wave velocity of the nearby stations and the generic shear-wave profile developed by Romero and Rix (2001).

Coefficients $a(1)$ through $a(12)$ are listed in Table 4-3 for each period. The last two columns of Table 4-3 present values of intra-event and inter-event standard deviation of the parametric model at each period. The sufficiency of the proposed model is investigated by plotting residuals against magnitude, V_{s30}, source to site distance for spectral periods of 0.0 (*PGA*) and 5.0 seconds in Figure 4-5. From Figure 4-5, one can observe that there is no apparent trend in the model residuals vs. different input parameters. Similar results for residuals are obtained for the regression analysis at other spectral periods.

Table 4-3. Coefficients a(1) through a(7) as well as standard deviation calculated for each period.

T(sec)	a(1)	a(2)	a(3)	a(4)	a(5)	a(6)	a(7)	a(8)	a(9)	a(10)	a(11)	σ_{inter}	σ_{intra}
0.001	0.8942	-0.3159	-0.0047	-0.9726	0.2399	2.0009	-0.5294	-0.2292	0.0263	0.0002	-0.4864	0.1916	0.0228
0.01	0.8899	-0.3019	-0.0073	-1.0066	0.2477	2.0905	-0.5529	-0.2576	0.0306	0.0002	-0.4864	0.1921	0.0221
0.02	0.6844	-0.1703	-0.0229	-1.0881	0.2629	2.4565	-0.6462	-0.3836	0.0483	0.0003	-0.4744	0.1977	0.0310
0.03	0.6747	-0.1303	-0.0241	-1.0808	0.2380	1.9555	-0.4769	-0.3018	0.0241	0.0002	-0.5088	0.2284	0.001
0.04	0.3008	-0.1644	0.0034	-0.4425	0.0768	0.2905	-0.0479	-0.0519	-0.0995	0.0005	-0.5772	0.2396	0.001
0.05	2.4925	-0.7073	0.0041	-1.8107	0.4215	1.7539	-0.3955	-0.0675	-0.0960	0.0004	-0.6015	0.2475	0.0986
0.075	1.7107	-0.5960	0.0160	-1.2491	0.2896	1.3608	-0.2899	0.1102	-0.0687	0.0002	-0.6896	0.2438	0.0913
0.1	0.4886	-0.1927	-0.0180	-0.7961	0.2082	0.5813	-0.1221	0.4239	-0.1059	0.0001	-0.5204	0.2355	0.1111
0.15	-0.1380	-0.0676	-0.0162	-0.4185	0.1289	0.4792	-0.1524	0.7409	-0.0462	-0.0003	-0.3799	0.2365	0.001
0.2	0.0254	-0.1939	0.0076	-0.2219	0.0794	1.0848	-0.2731	0.9104	-0.0322	-0.0005	-0.2189	0.2347	0.001
0.25	0.9652	-0.4696	0.0202	-0.6584	0.1792	0.9315	-0.1960	0.6888	-0.0440	-0.0003	-0.1423	0.2408	0.0361
0.3	0.9652	-0.4696	0.0202	-0.6584	0.1792	0.9315	-0.1960	0.6888	-0.0440	-0.0003	-0.1423	0.2408	0.0361
0.4	0.8499	-0.3031	-0.0052	-0.8217	0.2097	0.9371	-0.1906	0.6571	-0.0179	-0.0002	0.0182	0.2250	0.0453
0.5	1.7130	-0.6457	0.0295	-0.9929	0.2557	1.4105	-0.3322	0.7945	-0.0697	-0.0001	0.2048	0.2240	0.0420
0.75	3.0474	-1.2886	0.1083	-1.0069	0.2534	1.8040	-0.4618	0.9015	-0.1116	0.0000	0.1924	0.2301	0.0701
1	2.4202	-1.0605	0.0861	-0.8899	0.2331	2.4248	-0.6016	0.2296	0.0905	-0.0003	0.1115	0.2194	0.0616
1.5	1.3132	-0.7117	0.0667	-0.3595	0.1032	1.8621	-0.4432	0.4561	0.0946	-0.0007	0.0316	0.2211	0.0569
2	1.5714	-0.7427	0.0518	-0.7383	0.2151	2.7714	-0.6901	0.5451	0.0967	-0.0008	-0.0300	0.2160	0.0716
3	1.1085	-0.4419	0.0065	-0.8724	0.2463	2.7801	-0.7200	0.4254	0.1630	-0.0008	-0.0243	0.2097	0.0778
4	1.0275	-0.3558	-0.0070	-0.9609	0.2597	2.9565	-0.7784	0.0601	0.1894	-0.0005	-0.0435	0.2058	0.0674
5	1.2420	-0.4237	-0.0026	-1.0561	0.2801	3.0279	-0.7990	-0.0448	0.2027	-0.0005	-0.0882	0.2033	0.0579
7.5	1.2421	-0.4295	-0.0017	-1.0414	0.2759	2.8344	-0.7511	-0.0934	0.1902	-0.0004	-0.1464	0.1969	0.0506
10	1.3213	-0.4625	0.0012	-1.0805	0.2842	2.8719	-0.7569	-0.1407	0.1863	-0.0003	-0.1915	0.1911	0.0487

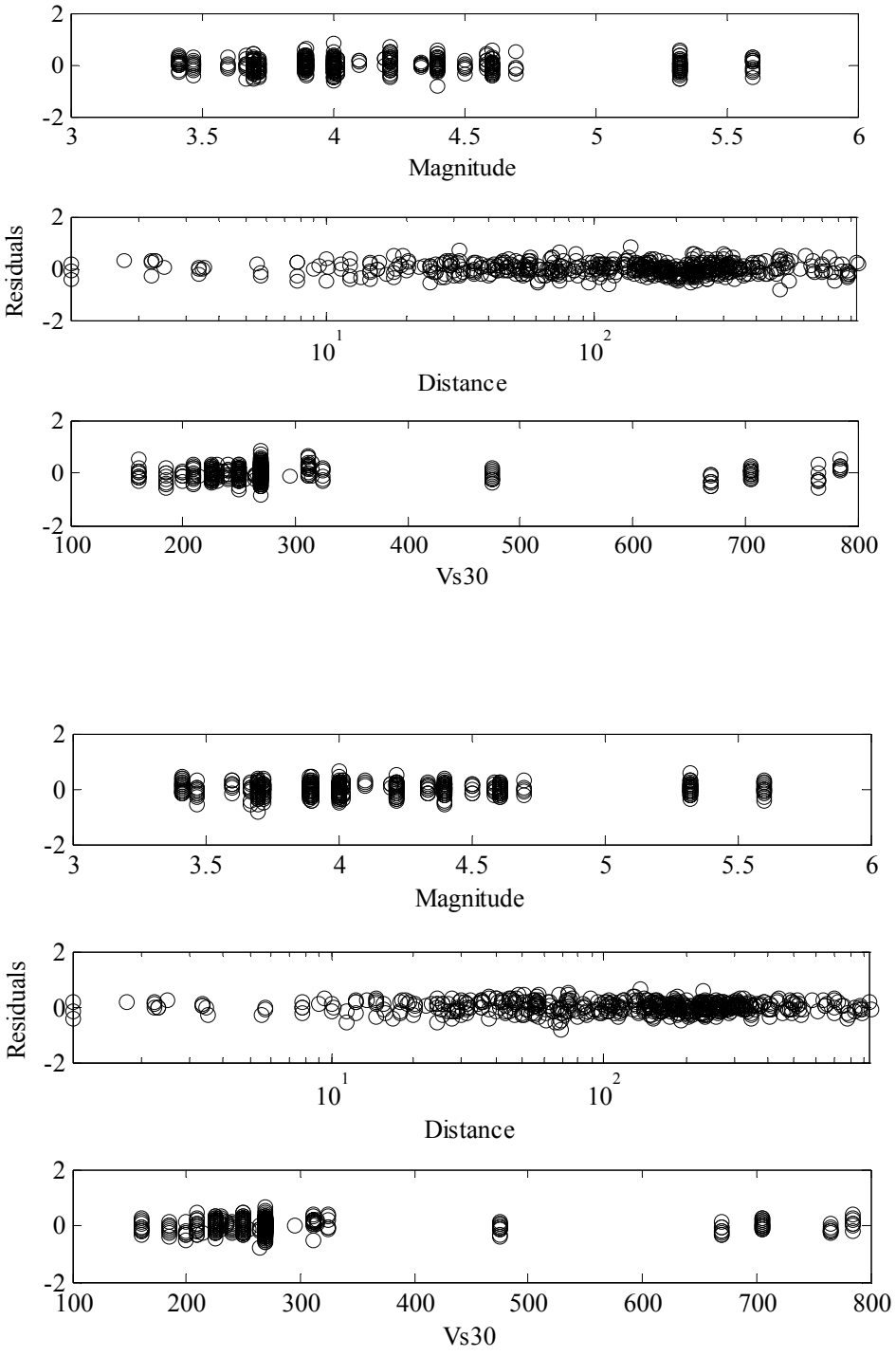

Figure 4-5. Residuals for *PGA* (top) and 1.0 seconds (bottom).

The median values for the V/H ratio for a site with a V_{s30} of 300 *m/s* and a rupture distance of 70 *km* are shown for 3 different magnitudes of 4.0, 5.0 and 6.0 in Figure 4-6. Predicted V/H ratios from Bommer et al. (2011), Gülerce and Abrahamson (2011), and McGuire et al. (2001) are also shown in Figure 4-6 for comparison. The McGuire et al. (2001) model is only available at the rock site conditions, which explains its distinct peak at very short periods. The median V/H ratio curves demonstrates the same expected shape with a peak in short period and a gradual increase from the minimum around 0.5 to 1.0 second. Figure 4-6 also demonstrates the dependence of the peak of the V/H ratio to magnitude.. In Figures 4-6 through 4-8, Bommer et al. (2011), Gülerce and Abrahamson (2011), and McGuire et al. (2001) models are graphed using *M=5*, *PGA*=0.4*g*, V_{s30} =300 *m/s*, *R*=100 *km,* and both the normal and the reverse fault types as input parameters.

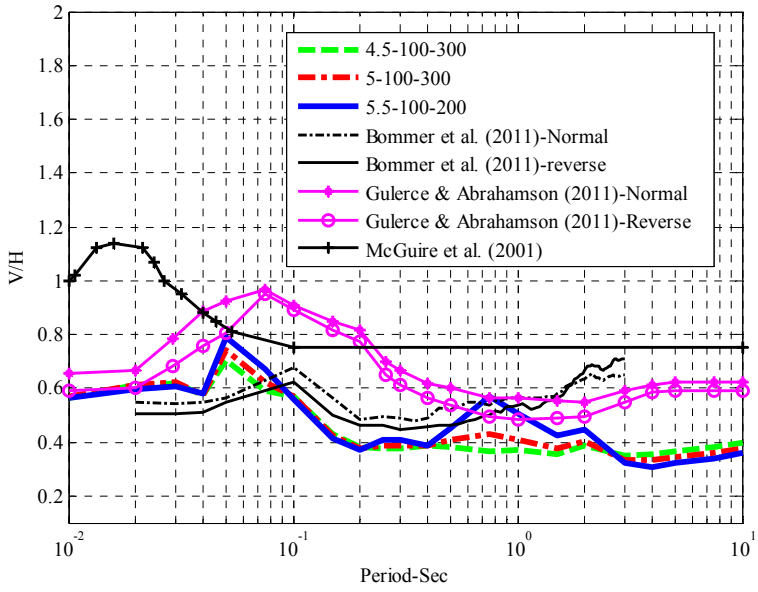

Figure 4-6. Effect of magnitude on the median values of V/H ratios for a site with a V_{s30} of 300 *m/s* and a rupture distance of 100 *km* and 3 different magnitudes of 4.5, 5.0 and 5.5. Predicted V/H ratios from Bommer et al. (2011), Gülerce and Abrahamson (2011), and McGuire et al. (2001) are graphed using M=5, *PGA*=0.4*g*, V_{s30} =300 *m/s*, R=100 *km*, and both the normal and the reverse fault types.

Figure 4-7 shows the effects of distance on the median values of V/H ratios. At long spectral periods, V/H ratios decreases with increasing source to site distance. Unlike long periods, where the effect of distance is dominant on the V/H ratios, at short periods distance has only a minor effect on the V/H ratio.

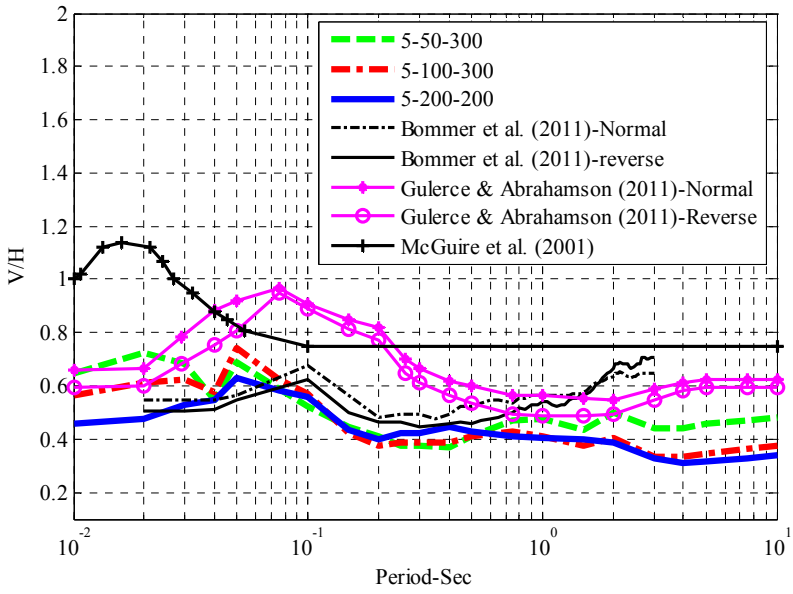

Figure 4-7. Effect of distance on the median values of V/H ratios for a site with a V_{s30} of 300 *m/s* and a rupture distance of 50, 150, and 250 *km* and magnitude of 5. Predicted V/H ratios from Bommer et al. (2011), Gülerce and Abrahamson (2011), and McGuire et al. (2001) are graphed using M=5, *PGA*=0.4*g*, V_{s30} =300 *m/s*, R=100 *km*, and both the normal and the reverse fault types.

Figure 4-8 illustrates predicted median values for V/H ratios of three different events with the same magnitude of 5 and source to site distance of 100 *km,* but for three different shear-wave velocities of 250,350, and 550 *m/s*. For the selected input parameters, V/H ratios decrease with increasing shear-wave velocity of sites for periods less than 0.4 seconds.

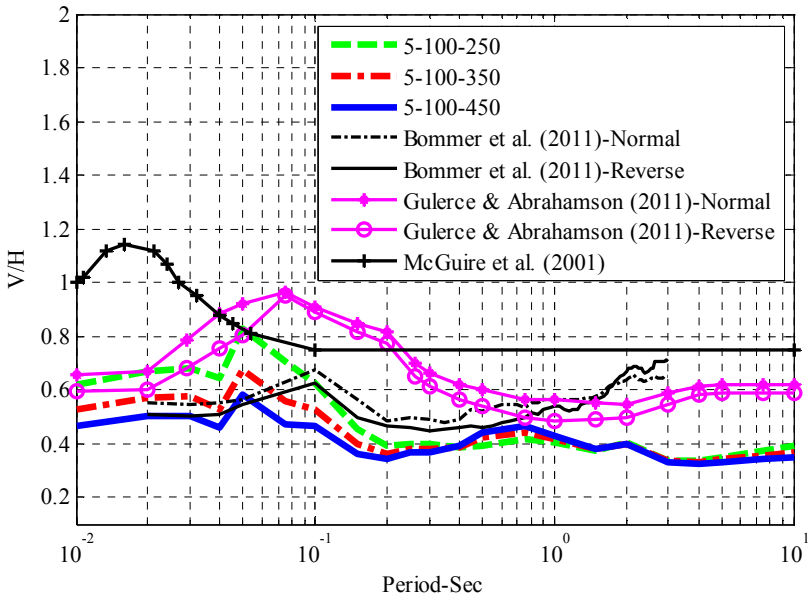

Figure 4-8. Effect of Vs30 on the median values of V/H ratios for a site with a V_{s30} of 250, 350, and 450 *m/s* and a rupture distance of 100 *km* and magnitude of 5. Predicted V/H ratios from Bommer et al. (2011), Gülerce and Abrahamson (2011), and McGuire et al. (2001) are graphed using M=5, *PGA*=0.4*g*, V_{s30} =300 *m/s*, R= 100 *km*, and both the normal and the reverse fault types.

4.5 Summary and Conclusions

A model to predict V/H ratios for the Mississippi embayment is presented in this study using 560 ground motion time-histories from 25 events. The presented model has the advantage of considering the dominant magnitude, source to site distance, and shear-wave velocity of soil deposits in the upper 30*m* of the site in a wide period range of 0.0 (*PGA*) to 10.0 seconds. A database of actual recordings from the CERI database and the NGA-East database with magnitudes ranging from 3.5 to 5.6 and distance ranging from 5 to 900 *km* is used in developing the V/H model. For applications outside the input magnitude and distance, the model should be used with caution.

The presented model, the only such model for the Mississippi embayment and the Central United States, has a general agreement with models suggested by Bommer et al. (2011) and Gulerece and Abrahamson (2011), which are based on data from the Western United States. Unlike the other two mentioned models, the proposed model does not include the type of faulting. The lower values of V/H resulting from my model are due to the difference between the tectonic and seismological differences between the Western and Central United States. Thick deposits of soil in the embayment causes large nonlinear effects, which are captured in the V/H analysis by using ground motion time-histories from stations inside the embayment.

4.6 References

Abrahamson, N. A., and Silva, W. J. (2008). "Summary of the Abrahamson and Silva NGA ground-motion relations." *Earthquake Spectra,* 24, 57-69.

Atkinson, G. M., (1993). "Notes on ground motion parameters for eastern north America: Duration and H/V ratio." *Bulletin of the Seismological Society of America,* 83(6), 1778-1798.

Bakun, W. H. and Hopper, M. G. (2004). "Magnitudes and Locations of the 1811-1812 New Madrid, Missouri, and 1866 Charleston, South Carolina, earthquakes." *Bulletin of the Seismological Society of America,* 94(1), 64-75.

Bommer, J. J., Akkar, S., and Kale, O. (2011). "A Model for Vertical-to-Horizontal Response Spectral Ratios for Europe and the Middle East." *Bulletin of the Seismological Society of America,* 101(4), 1783-1806.

Bozorgnia, Y. and Campbell K. W. (2004a). "Engineering characterization of ground motion, in Earthquake Engineering: From Engineering Seismology to Performance-Based Engineering." Y. Bozorgnia and V. V. Bertero (Editors), CRC Press, Boca Raton, Florida, 215-315.

Cramer, C. H. (2011). "Next Generation Attenuation East Initial Flat Files for Eastern North America." Report to NGA-East working group.

Cramer, H. C. and Boyd, O. S. (2011). "Why the New Madrid Earthquakes are M7–8 and the Charleston Earthquake is ~M7." Report to USGS.

Eurocode 8 (2009). "Design of structures for earthquake resistance, part 1: General rules, seismic actions, and rules for buildings." EN 1998-1, European Committee for Standardization (CEN), http://www.cen.eu/ cenorm/homepage.htm.

Gülerce, Z., and Abrahamson, N. A. (2011). "Site-specific spectra for vertical ground motion." *Earthquake Spectra*, 27, no. 4 (in press).

Joyner, W. B. and Boore, D. M. (1993). "Methods for regression analysis of strong-motion data." *Bulletin of the Seismological Society of America*, 83, 469-487.

Kunnath, S. K., Erduran, E., Chai, Y. H., and Yashinsky, M. (2008). "Effect of near-fault vertical ground motions on seismic response of highway overcrossings." *Journal of Bridge Engineering*, ASCE, 13, 282-290.

Lermo, J., and Chávez-García F., (1993). "Site effect evaluation using spectral ratios with only one station." *Bulletin of the Seismological Society of America,* 83, 1574-1594.

McGuire, R. K., Silva W. J., and Costantino C. J. (2001). "Technical basis for revision of regulatory guidance on design ground motions: Hazard and risk-consistent ground motion spectra guidelines." U.S. Nuclear Regulatory Commission NUREG/CR-6728, Washington, D.C., 1020 pp.

Nakamura, Y. (1989). "A method for dynamic characteristics estimation of subsurface using microtremor on the ground surface." *Quarterly Report of Railway Technical Institute (RTRI),* 30, 25–33.

National Earthquake Hazards Reduction Program (NEHRP; 2009). 2009 NEHRP recommended seismic provisions for new buildings and other structures. Part 1, Provisions, National Earthquake Hazards Reduction Program, Washington D.C., 373 pp.

Pezeshk, S., Zandieh A., and Tavakoli B. (2011). "Hybrid Empirical Ground-Motion Prediction Equations for Eastern North America Using NGA Models and Updated Seismological Parameters." *Bulletin of the Seismological Society of America*, 101(4), pp.1859-1870.

United States Atomic Energy Commission (USAEC; 1973). "Design response spectra for seismic design of nuclear power plants, Regulatory Guide R. G. 1.60." Atomic Energy Commission, Washington.

Walling, M., Silva, W., and Abrahamson, N. A. (2008). "Nonlinear site amplification factors for constraining the NGA models." *Earthquake Spectra,* 24, 243–255.

Zandieh, A. and Pezeshk S. (2011). "A Study of Horizontal-to-Vertical Component Spectral Ratio in the New Madrid Seismic Zone." *Bulletin of the Seismological Society of America,* 101(1), 287–296.

5 Conclusions

Three topics in the field of geotechnical seismic engineering and engineering seismology are discussed in this manuscript. In the first part of this dissertation, using analytical data from nonlinear site response analyses for several cases, a parametric site response model was developed for the Mississippi embayment as a function of *PGA* on the reference bedrock, V_{s30}, depth of soil columns, and geology. The nonlinear response of the soil column was computed using the computer program NOAH, which takes into account the pore water pressure development in soil media. The proposed model consists of three different functional forms, to take into account the unique features of the study area such as thick deposits of soil, variable bedrock depth, and having two dominant geological structures.

This study shows that the site amplification within the Mississippi embayment is relatively high, especially at low periods and low *PGA*s, in comparison with the proposed values of the NEHRP, Choi and Stewart (2005), and Walling et al. (2008), which are derived with data from the west coast. Geology also has a considerable role in the site response of the study area when the bedrock depth is relatively shallow. The effect of geology decreases as the depth of the bedrock increases. At long periods, the Mississippi embayment shows no nonlinearity in the ground motion amplification, which is consistent with findings of other studies (the NEHRP, Choi and Stewart 2005, and Walling et al. 2008); but the predicted value of ground motion amplification is substantially higher in comparison with values of the NEHRP, Choi and Stewart (2005), and Walling et al. (2008) due to the effects of deep soil deposits.

In the second part of the dissertation, a new step-by-step method is developed to select a set of ground motions for time-history analysis of structures that takes into account a site-specific PSHA and the associated uncertainties. In the developed method, epistemic uncertainties of the study site are captured by using multiple individual targets in ground motion selection steps. In the proposed method, after capturing the variability of the UHRS, a Monte Carlo procedure is used to produce a set of response spectra that has a mean equal to the target and variability close to the variability of the target at all the spectral periods by performing a separate PSHA for each branch of the logic tree. Each member of the generated set is called an individual target response spectrum, and ground motions from a database are selected based on their similarity with the individual target response spectra. I selected acceleration time-histories from a database of real ground motions, as well as ground motions produced using synthetic methods: a point-source stochastic procedure and records generated using a stochastic finite-fault model. Databases of synthetic ground motions have the advantage of reflecting seismological parameters of the region assuming databases of real ground motions are not from the region of interest. The method's procedure is defined through studying a sample site in North of the Mississippi embayment.

In the last part of this dissertation, a model for the V/H ratio of 5% damped spectral acceleration is proposed for the Mississippi embayment. The resultant V/H ratio model can be used to scale the available horizontal design spectrum to the vertical site-specific design spectrum. The presented model, the only such model for the Mississippi embayment and the Central United States, has a general agreement with models suggested by Bommer et al. (2011) and Gülerce and Abrahamson (2011), which are

based on the data from the Western United States. The predicted peak of the V/H ratio for the study area is around 0.05 second which is not dependent on site conditions. At long periods the values of V/H ratio fall below other models and are around 0.5. The proposed model predicts lower values of V/H ratio at *PGA* in comparison with the McGuire et al. (2001), model which is developed for rock site conditions. The values of V/H ratio at *PGA* are between 0.45 and 0.65 which is closer to the values predicted by the Gülerce and Abrahamson (2011) and the Bommer et al. (2011) models. The effect of the shear-wave velocity of a site decreases with increasing spectral period.

One limitation of the proposed model is lack of large magnitude events in the database. Only one event with moment magnitude of 5.6 is present in the database and makes the resulting coefficients dependent on data from one event.

6 Future Work

An important element missing in the first part of this dissertation is the effect of propagated ground motions on the resulting parametric model. Possible future work would be to estimate site response using ground motion other than those generated by the SMSIM program, such as actual data from the recently developed NGA-East database. This database consists of data from world-wide earthquakes that have seismological parameters similar to the seismological parameters of the Central and Eastern United States. A database from other synthetically simulated ground motions such as finite-fault models, which take into account the near-fault effects, can also be used to investigate the effect of a particular database on ground motion amplification. Using a better estimate of soil properties such as shear modulus degradation and damping curves for the study area would be a great improvement in making the results of site response analysis closer to reality.

A complement to the second part of my dissertation would be to perform a time-history analysis on a sample structure using the proposed method, and to compare the structural response (*e.g.,* maximum inter-story drift ratio, maximum axial forces of columns, etc.) with the results of other ground motion selection methods. From a structural standpoint, a ground motion selection and scaling approach should result in an unbiased estimate of different structural responses.

With the help of the CERI network and other regional seismic networks such as EarthScope's Transportable Array (TA arrays), more data are available after each major event. The database used in this research can be updated with the time-histories of the new events in the region to better constrain the model, especially for events larger than

magnitude 5.6. To be more precise, the event with longitude and latitude of 35.20° and -90.63° and the occurrence date of 10/29/2012 was not included in the database used to predict the model coefficients in chapter three.